VASCULAR STABILITY, BARRIER FUNCTION, AND DISEASE

by

Tara Mariella Mleynek

A dissertation submitted to the faculty of
The University of Utah
in partial fulfillment of the requirements for the degree of

Doctor of Philosophy

Department of Oncological Sciences

The University of Utah

May 2015

The University of Utah Graduate School

STATEMENT OF DISSERTATION APPROVAL

The dissertation of **Tara Mariella Mleynek**

has been approved by the following supervisory committee members:

Dean Li	, Chair	**August 20 2014** Date Approved
Jody Rosenblatt	, Member	**August 20 2014** Date Approved
Charles Murtaugh	, Member	**August 20 2014** Date Approved
Katharine Ullman	, Member	**August 20 2014** Date Approved
Bryan Welm	, Member	**August 20 2014** Date Approved

and by **Bradley Cairns** , Chair/Dean of

the Department/College/School of **Oncological Sciences**

and by David B. Kieda, Dean of The Graduate School.

ABSTRACT

Endothelial cells exist in a state of dynamic stability allowing for a balance between quiescence and response. These cells create the barrier system of the vasculature as well as drive the growth of new vessels. The disease Cerebral Cavernous Malformation (CCM) disrupts both processes and is characterized by leaky, cavernous vascular lesions in the CNS, resulting in headache, seizure, and stroke. CCM occurs in both a sporadic and familial form thought to follow the Knudsen two-hit model of retinoblastoma. Studies have been primarily focused on late stage disease, leaving little understanding of the earliest stages and the precise role of the second hit. We sought to study early developmental onset to identify morphological characteristics that could provide mechanistic insight to the key initiating factors.

We generated an inducible endothelial knockout mouse model of CCM and found that when the second hit occurs at birth, mice develop cavernous malformations in the brain and the retina. We determined that lesions arise in a spatially and temporally predictable pattern in a limited developmental window. We further showed vessel defects are preceded by endothelial hypersprouting and an impaired cellular response to flow. In the context of CCM, this suggests that an inability of cells to react to their environment could result in lesion development. Our findings that loss of the second hit in adulthood was insufficient to cause disease, combined with the predictable nature of development,

suggested that environmental factors may be necessary contributors to disease onset. While loss of the genetic hits in adulthood was not enough to cause disease we found that, when combined with localized vascular endothelial growth factor (VEGF), lesions can arise.

Changes in the surrounding tissue environment can be caused by disrupted barrier functions, promoting a disease state like that seen in CCM. In our pursuit to further understand barrier function in the face of environmental challenges, we defined the novel process of endothelial extrusion. Extrusion is the removal of an apoptotic cell from a monolayer, prior to its structural collapse, via contraction of an actin ring. Together these studies offer insights into endothelial barrier function, stability, and disease.

This dissertation is dedicated to Jack Mleynek, who led me to this path and encouraged me throughout the journey.

“Be a man.” – Aubrey Chan

TABLE OF CONTENTS

LIST OF FIGURES

Figures

ACKNOWLEDGEMENTS

I would like to thank the people who contributed to this work. First and foremost I would like to thank my mentor Dean Li, who taught me so much at and away from the bench, and whose drive and intelligence will remain an inspiration. I would like to thank my committee members for their advice and guidance: Jody Rosenblatt, Charlie Murtaugh, Katie Ullman, and Bryan Welm. I would also like to thank all the members of the Li lab family: Aubrey Chan, Kirk Thomas, Chadwick Davis, Dallas Shi, Christopher Gibson, Jae Hyuk Yoo, Lise Sorensen, Jing Ling, Shannon Odelberg, Weiquan Zhu, Matt Smith, Nyall London, Aaron Rogers, and Meghan Wooley. Let me not forget all the others who have helped me along the way: Kevin Whitehead, Kandis Carter, Mike Redd, Chris Rodesch, Mike Bridge, George Eisenhoffer, Yapeng Gu, Tom Marshall, and Osama Abdulla. Finally, my husband, Darren, thank you for the love, the support, and the new perspective.

CHAPTER 1

INTRODUCTION

The vascular system spans the entire body as a vast, branching network that pervades most tissues. This network is comprised of interconnected large arteries and veins, which expand into arterioles and venoules and finally extend into labyrinths of small capillaries. Each blood vessel is comprised of layers of connective tissue, support cells, and endothelial cells (Figure 1.1). The thickness of each layer reflects the function of the vessel. For example, arteries are large, central vessels that transport ample volumes of blood under high pressure. As such, arteries have more support cells and connective tissue. In contrast, capillaries operate under lower pressure in a diffuse network; therefore the amount of support cells and connective tissue needed is much less. Regardless of vessel function however, the inner lining of endothelial cells is always present (1, 2).

In capillaries, the endothelial lining exists in a monolayer. Despite its single-cell thickness, this monolayer is responsible for several processes of vascular biology. It is in the capillary beds that endothelial cells enact their role as gatekeepers of the blood-tissue barrier and allow for the selective passage of matter such as nutrients and oxygen (3). These cells join together via several junction contacts between one another. One of the

most well characterized junction proteins is Vascular Endothelial Cadherin, VE-Cadheren, which plays an essential role in establishing and maintaining the endothelial barrier. Increasing or decreasing levels of VE-Cadherin between the cells can increase or decrease the strength of the endothelial barrier, respectively (4). In addition to joining with each other, endothelial cells are connected to the basement membrane via transmembrane adhesion molecules known as integrins. The basement membrane is a laminin-rich matrix that provides additional support and organization for the endothelial cells (5). An established endothelial monolayer can then act as a platform for new vascular growth via the process of angiogenesis

Angiogenesis is the creation of new vessels and begins when an endothelial cell responds to growth factors produced by the nearby tissue microenvironment. The responding cell, referred to as a tip cell, becomes migratory and begins to extend sprouts. The tip cell then signals to its neighbors, inducing them to become support cells that will form the endothelial network trailing behind the tip cell. These support cells, referred to as stalk cells, proliferate, lumenize, and aid in recruiting vascular smooth cells in order to generate the new vascular network (6-8).

Once the vascular network has been established, the endothelial cells enter into a state of quiescience and go on to execute their role in barrier function. This barrier of endothelial cells selectively allows for the passage of nutrients, cells, and fluid while maintaining the structural integrity of the separate tissue compartments.

Dysfunction within the endothelium has been attributed to several diseases of the vasculature. For example, a disruption in appropriate VE-Cadherin signaling and junction localization can result in a less effective barrier. This may contribute to the formation of

rheumatoid arthritis by increasing vascular permeability within synovial joints, allowing fluid and inflammatory cells to leak into the tissue (9). Another example of endothelial dysfunction and disease can be seen with the disruption of angiogenic regulation in diabetic retinopathy. In this disease, inappropriate growth factor secretion and response by the endothelial cells results in inappropriate neovascularization within the retina (10). Different types of endothelial dysfunction will subsequently lead to different disease states, often involving crossover of many endothelial signaling pathways. One prominent example of vascular disease involving dysregulation of both barrier function and angiogenesis is vascular malformations.

Vascular malformations are defects in normal vascular structure. Healthy vascular structure is one of ordered, sequential vascular branches that form organized networks of lumenized vessels allowing for proper blood flow and transport. In the case of vascular malformations, the architecture is disrupted such that select areas develop into tortuous, dilated entaglements of improperly lumenized vessels. There are several different types of vascular malformations, each with their own unique architecture and endothelial defects. These include arteriovenous malformations, telangectasias, venous malformations, and cavernous hemangiomas (11). The presence of cavernous hemangiomas is the hallmark of the disease Cerebral Cavernous Malformation (CCM) (Figure 1.2). The vascular malformations that develop in CCM primarily arise in the brain and are characterized by clusters of vascular caverns that lack any intervening brain parenchyma, giving them a raspberry-like structure (12). The lesions themselves, thought to be of capillary origin, are comprised of a thin-walled layer of endothelium that lacks smooth muscle support and is surrounded by fibrosis. Blood can fill into the caverns and,

due to the compromised structure and inherent endothelial dysfunction, can leak into the surrounding brain tissue. This can lead to headaches, seizure, and stroke for those with the disease (13). CCM affects 0.5% of the population and can occur sporadically or can be inherited in an autosomal dominant pattern. The inherited form of the disease is caused by the loss of function in one of three genes: CCM1, CCM2, and CCM3 (14-16).

Each of these proteins is thought to act as a scaffold, and all have been shown to bind together in a complex and can interact with several other unique signaling partners. None of the proteins are known to have enzymatic activity (17). CCM1, also known as Krev interaction trapped protein 1 (Krit1), was first identitified in a yeast-two hybrid screen for Rap1 effectors. Rap1 binding to CCM1 stabilizes VE-Cadherin at the cell junctions (18). Without CCM1, these junctions become disorganized (19). Additional consequences of loss of CCM1 include activation of β1-integrin, dysregulation of Notch signaling, and increased levels of reactive oxygen species, implying a complex role for this gene in cell signaling (17). A recent report identified the TGF-β pathway as a major player in pathogenesis in the absence of CCM1. The subsequent increase in TGF-β and BMP6 induced endothelial to mesenchymal transition in brain endothelial cells, contributing to the formation of vascular malformations (20). In addition to these signaling roles, CCM1 is important in cytoskeletal dynamics much like CCM2 (21).

At first known as osmosensing scaffold for MEKK3 (OSM), CCM2, was originally identified in a yeast-2-hybrid screen for MEKK3 binding partners. Upon stress signaling, CCM2 activates various mitogen activating protein kinases (MAPKs) such as p38 and JNK (22). CCM2 can also activate the Rho GTPases and has been shown to bind to RhoA. In the absence of CCM2, cells upregulate the activity of RhoA leading to the

formation of intracellular actin stress fibers (21). These stress fibers disrupt normal cell morphology, which in turn leads to a decrease in endothelial barrier function (23).

In contrast to both CCM1 and CCM2, CCM3 has not been implicated in the activity of RhoA. CCM3, known also as programmed cell death 10 (PDCD10), was identified for its role in apoptosis of cultured premyeloid cells. Endothelial cells lacking CCM3 do not exhibit the same cytoskeletal defects a seen in cells missing CCM1 or CCM2 (24). Instead, CCM3 is required for appropriate establishment of golgi polarity, dependent upon the binding of PDCD10 to the proteins in the germinal center kinase (GCK) family (17) (Table 1).

Despite the apparent different biochemical functions of these three proteins, mutations in any one of their encoding genes results in phenotypically similar disease states, suggesting that a common convergent mechanism is at play (24). While the sporadic form of the disease gives rise to singular lesions and progresses at a slow rate, the inherited form of the disease is more aggressive, usually presenting with multiple lesions that progress rapidly. This disease pattern resembles that seen in the rare cancer, retinoblastoma. Retinoblastoma also occurs in a sporadic and inherited form, with the inherited form being much more severe. Alfred Knudson in 1971 made the proposition that, based on clinical data, multiple "hits" to normal cellular function were required to induce disease. In familial disease, the first hit is the inherited mutation, and acquisition of the second hit would rapidly lead to cancer. The sporadic form, however, would require two somatic hits (25). This type of mechanism is known as the Knudson two-hit hypothesis, and evidence from CCM patients support a similar mechanism to explain CCM. Surgically excised tissue from patients with familial CCM were shown to contain

not only their inherited, germline mutation, but an additional mutation in the other CCM allele, implying that endothelial cells within CCM lesions had acquired a second genetic hit much as Knudson proposed (26, 27).

In order to study the pathogenesis of CCM and whether the two-hit model applies, numerous mouse models have been generated. Initial models included creating germline knockouts for the CCM genes. Mice homozygous for any of a deleted CCM allele failed to survive past embryonic development, while mice that were heterozygous went on to survive through adulthood with no apparent vascular defects (21, 28, 29). These initial models, while supportive of the hypothesis that loss of heterozygosity was needed for CCM disease, were not ideal for disease study. While the death of the germline homozygous knockouts was attributed to failed vascular development, these mice were insufficient to address whether the loss of CCM led to brain lesion formation or how the two-hit model might be at play. Therefore additional models needed to be created that allowed for mice to survive beyond birth. The first model took advantage of the heterozygous CCM1 loss of function mouse that was also homozygous for a mutation in p53. While mice heterozygous for CCM1 do not form any sort of vascular anomalies, the homozygosity at p53 promotes genetic instability, increasing the mutation rate and thus increasing the chance of the loss of the second CCM1 allele. These mice did go on to develop CCM lesions (30). A similar approach was conducted by McDonald et al. using a mismatch repair deficient mouse, Msh2, in lieu of the p53 mutant mouse. Similar results were obtained for CCM1; however, when done with CCM2, mice failed to develop any type of lesion (31). While these models provided interesting insight and supported the two-hit hypothesis, these models were not fully penetrant, and only a subset of the

populations developed malformations. In addition, the inherent genetic instability of the models led to the development of other non-CCM mutations as well as to the development of tumors. Both of these factors skew the ability to test the specific role that loss of the CCM genes play in disease.

An alternative method, less reliant on serendipitous genetic modification, has been employed by a number of laboratories. This approach takes advantage of an inducible transgene encoding the Cre recombinase to mutate the second CCM allele at a time and in tissues determined by the investigator (20, 24, 29). These Cre models allowed for a more reliable induction of disease that faithfully recapitulated human disease progression and anatomical pathology (24).

Such models have allowed a more detailed exploration into cellular mechanisms disrupted following the second genetic hit and offer hope for the development of pathway-specific therapeutics. A recent report using an inducible model of CCM1 implicated the TGF-β pathway in disease progression and has prompted attempts to treat CCM disease with TGF-β inhibitors. While moderately effective, the treatment did not completely rescue the disease phenotype, and lesions still developed (20). Another study, spurred by a mouse model of CCM2 disease, tested the efficacy of the Rho inhibitor Fasudil, but it resulted in limited success (32). Despite the moderate promise seen with these drugs, it highlights a critical limited focus of current CCM research. Such research is primarily focused on late stage disease, after lesions have been well established. While this has yielded exciting results via the identification of novel pathways, it raises the risk of confusion between primary effects and secondary effects associated with the extended disease process. Signal cascades that are disrupted in mature disease states may not be

those responsible for its onset, raising the likelihood of drugs developed to a symptom and not the cause. Understanding how this two-hit mechanism impacts vascular development and the early pathophysiology of the disease would allow for identification of primary pathways, opening the door for more discerning treatment options.

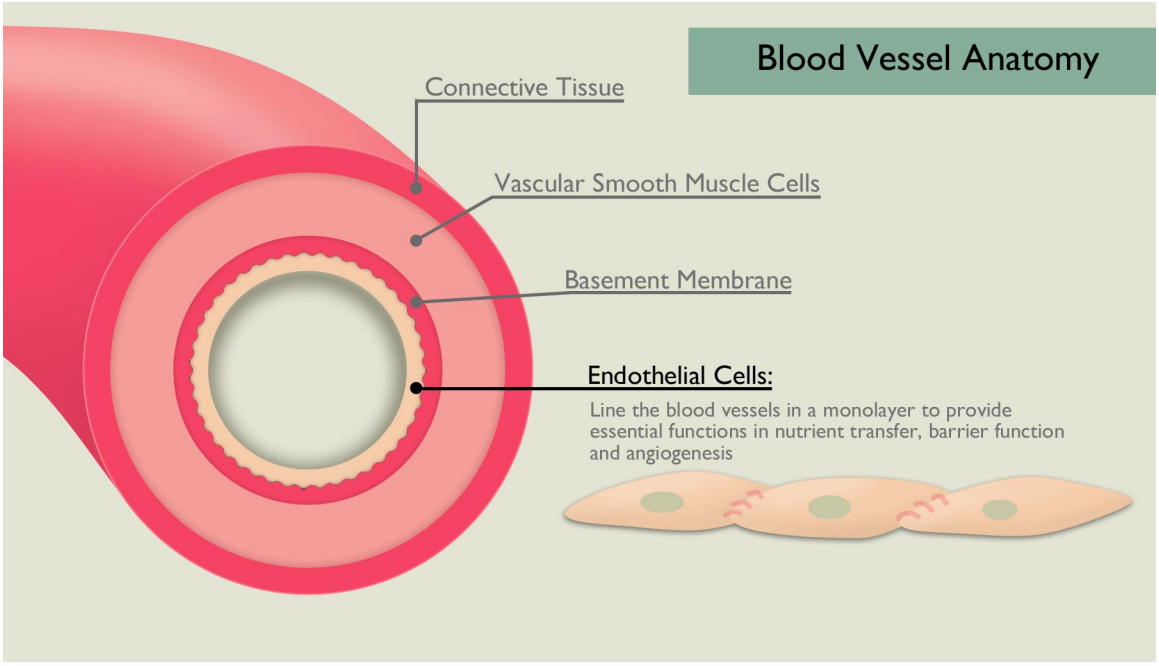

Figure 1.1: The basic anatomy of a blood vessel. Blood vessels are comprised of multiple distinct layers, each with its own composition. The outer most layer is primarily constructed from connective tissue and is adjacent to a layer of smooth muscle cells. The smooth muscle cells provide support for the inner most layer of endothelial cells, which are anchored to a basement membrane. It is the endothelial cells that carry out functions in selective transport and barrier control.

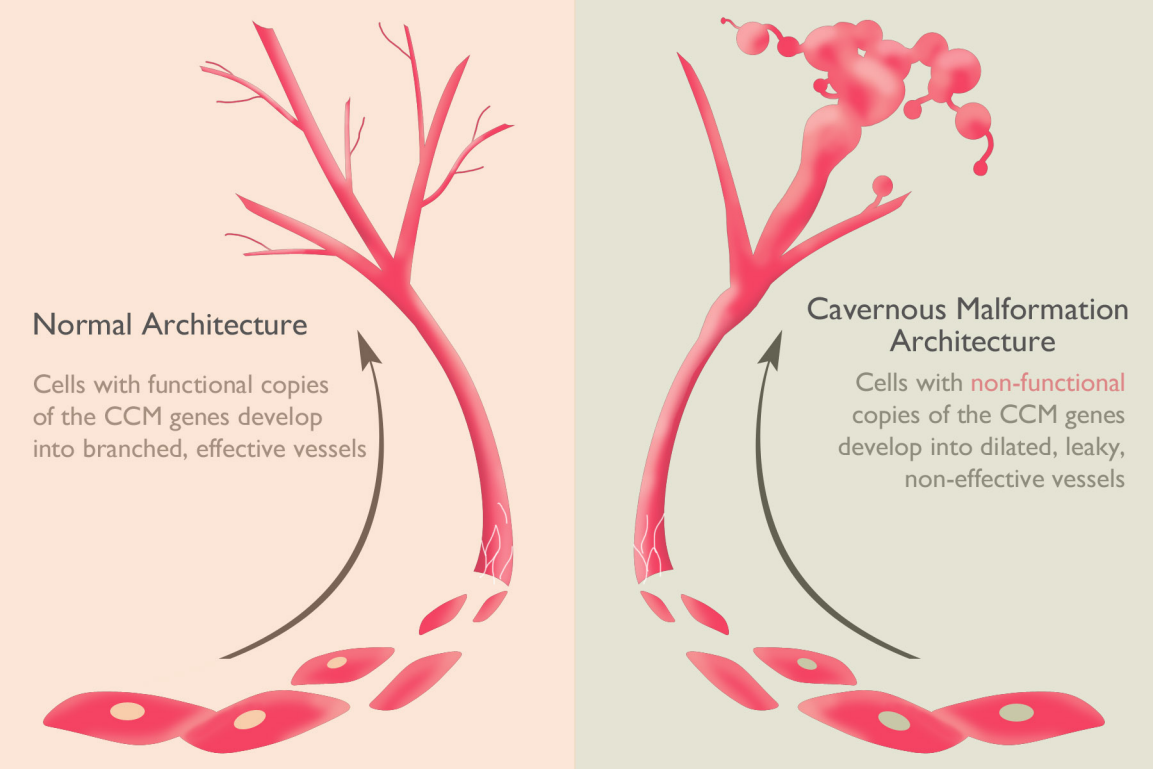

Figure 1.2: Comparison of normal vascular architecture to that of cavernous malformation architecture. Typical vascular structure is one of successive branching with larger vessels splitting into smaller vessels until the capillary bed. These vessels have a patent lumen allowing for adequate blood flow. In the case of cavernous malformations, the branching structure is replaced by chaotic entanglements. The entanglements are comprised of bulbous vascular sacs that are thin-walled, causing blood to pool and leak, rather than flow.

Table 1.1: Summary of CCM proteins (17, 20, 24, 33)

Name	CCM1 (Krit1)	CCM2 (OSM, Malcavernin)	CCM3 (PDCD10)
Size	736 AA	444 AA	212 AA
Binding Domains	Nudix(N), NPxY/F, Ankryin, FERM(C)	PTB(N), HHD(C)	Dimerization domain(N), FAT-H(C)
Binding Partners	CCM2, CCM3, Rap1 ICAP1, HEG-1,Microtubules	CCM1, CCM3, Rho, RAC-1 MEKK3, SMURF-1	CCM1, CCM2, paxillin, STRIPAK, GCKIII family, VEGFR2
Consequence of loss on cell signaling	Increased TGFB, integrin, Rho, and ROS; disregulated Notch and VE-Cadherin	Increased Rho, pMLC2, JNK, MKK4, MKK7	Decreased VEGFR2, p38, and apoptosis
Consequence of loss on cell phenotype	Decreased barrier function Failed lumenization Disrupted polarity, junctions		

1.1 References

1 Udan, R.S., Culver, J.C. and Dickinson, M.E. (2013) Understanding vascular development. *WIREs Dev. Biol.*, **2**, 327-346.

2 Alberts, B., Johnson, A., Lewis, J., Raff, M., Roberts, K. and Walter, P. (2002). *Molecular Biology of the Cell*. 4th edition. Garland Science, New York.

3 Galley, N.W. (2004) Physiology of the endothelium. *Brit. J. Anaesth.*, **93**, 105-113.

4 Hordijk, P. L., Anthony, E., Mul, F. P. J., Rientsma, R., Oomen, L. C. J. M. and Roos, D. (1999) Vascular-endothelial-cadherin modulates endothelial monolayer permeability. *J. Cell Sci.*, 1915-1923.

5 Davis, G.E. (2005) Biosynthesis, remodeling, and functions during vascular morphogenesis and neovessel stabilization. *Circ. Res.*, 1093-1107.

6 Bentley, K., Mariggi, G., Gerhardt, H. and Bates, P.A. (2009) Tipping the balance: robustness of tip cell selection, migration and fusion in angiogenesis. *PLOS Comput. Biol.*, **5**, e1000549.

7 Gerhardt, H., Golding, M., Fruttiger, M., Ruhrberg, C., Lundkvist, A., Abramsson, A., Jeltsch, M., Mitchell, C., Alitalo, K., Shima, D. *et al.* (2003) VEGF guides angiogenic sprouting utilizing endothelial tip cell filopodia. *J. Cell Biol.*, **161**, 1163-1177.

8 Tung, J.J., Tattersall, I.W. and Kitajewski, J. (2012) Tips, stalks, tubes: notch-mediated cell fate determination and mechanisms of tubulogenesis during angiogenesis. *Cold Spring Harb. Perspect. Med.*, **2**, a006601.

9 Zhu, W., London, N.R., Gibson, C.G., Davis, C. T., Tong, Z.Z., Sorensen, L.K., Shi, D.S., Guo, J., Smith, M. C. P., Grossmann, A. H. *et al.* (2012) Interleukin receptor activates a MYD88–ARNO–ARF6 cascade to disrupt vascular stability. *Nature*, 252-255.

10 Caldwell, R.B., Bartoli, M., Behzadian, M.A., El-Remessy, A.E., Al-Shabrawey, M., Platt, D. H. and Caldwell, R. W. (2003) Vascular endothelial growth factor and diabetic retinopathy: pathophysiological mechanisms and treatment perspectives. *Diabetes Metab. Res. Rev.*, 442-455.

11 Leblanc G.G., Davis, G.E., Awad, I.A. and Young, W.L. (2009) Biology of vascular malformations of the brain, NINDS Workshop Collaborators. *Stroke*, **40**, 694-702.

12 Otten, P., Pizzolato, G.P., Rilliet, B. and Berney, J. (1989) A study of 131 cases of

cavernomas of the cns, discovered on retrospective analysis of 24,535 autopsies. *Neurochirurgie*, **35**, 82-83.

13 Clatterbuck, R.E., Eberhart, C.G. and Rigamonti, D. (2001) Ultrastructural and immunocytochemical evidence that an incompetent blood-brain barrier is related to the pathophysiology of cavernous malformations. *J. Neurol. Neurosurg. Psychiatry*, **71**, 4.

14 Robinson, J.R., Awad, I.A. and Little, J.R. (1991) Natural history of the cavernous angioma. *J. Neurosurg.*, **75**, 5.

15 Vernooij, M.W., Ikram, M.A., Tanghe, H.L., Vincent, A.J., Hofman, A., Krestin, G.P., Niessen, W.J., Breteler, M.M. and van der Lugt, A. (2007) Incidental findings on brain MRI in the general population. *N. Engl. J. Med.*, **357**, 7.

16 Plummer, N.W., Zawistowski, J.S. and Marchuk, D.A. (2005) Genetics of cerebral cavernous malformations. *Curr. Neurol. Neurosci.*, **5**, 5.

17 Draheim, K.M., Fisher, O.S., Boggon, T.J. and Calderwood, D.A. (2014) Cerebral cavernous malformation proteins at a glance. *J. Cell Sci.*, in press., 1-7.

18 Glading, A., Han, J., Stockton, R.A. and Ginsberg, M.H. (2007) KRIT-1/CCM1 is a Rap1 effector that regulates endothelial cell cell junctions. *J. Cell Biol.*, **179**, 247-254.

19 Lampugnani, M.G., Orsenigo, F., Rudini, N., Maddaluno, L., Boulday, G., Chapon, F. and Dejana, E. (2010) CCM1 regulates vascular-lumen organization by inducing endothelial polarity. *J. Cell Sci.*, **123**, 1073-1080.

20 Maddaluno, L., Rudini, N., Cuttano, R., Bravi, L., Giampietro, C., Corada, M., Ferrarini, L., Orsenigo, F., Papa, E., Boulday, G. *et al.* (2013) EndMT contributes to the onset and progression of cerebral cavernous malformations. *Nature*, **498**, 492-499.

21 Whitehead, K.J., Chan, A.C., Navankasattusas, S., Koh, W., London, N.R., Ling, J., Mayo, A.H., Drakos, S.G., Jones, C.A., Zhu, W. *et al.* (2009) The cerebral cavernous malformation signaling pathway promotes vascular integrity via Rho GTPases. *Nat. Med.*, **15**, 177-184.

22 Uhlik, M.T., Abell, A.N., Johnson, N.L., Sun, W., Cuevas, B.D., Lobel-Rice, K.E., Horne, E.A., Dell'Acqua, M.L. and Johnson, D.L. (2003) Rac–MEKK3–MKK3 scaffolding for p38 MAPK activation during hyperosmotic shock. *Nat. Cell. Biol.*, **5**, 1104-1110.

23 Wójciak-Stothard, B., Potempa, S., Eichholtz, T. and Ridley, A.J. (2001) Rho and Rac but not Cdc42 regulate endothelial cell permeability. *J. Cell. Sci.*, **114**, 1343-1355.

24 Chan, A.C., Drakos, S.G., Ruiz, O.E., Smith, A.C., Gibson, C.C., Ling, J.,

Stratman, A.N., Sacharidou, A., Revelo, M.P. *et al.* (2011) Mutations in 2 distinct genetic pathways result in cerebral cavernous malformations in mice. *J. Clin. Invest.*, **122**, 5.

25 Knudson, A.G. Jr. (1971) Mutation and cancer: statistical study of retinoblastoma. *Proc. Natl. Acad. Sci. USA*, **68**, 820-823.

26 Akers, A.L., Johnson, E., Steinberg, G.K., Zabramski, J.M. and Marchuk, D.A. (2009) Biallelic somatic and germline mutations in cerebral cavernous malformations (CCMs): evidence for a two-hit mechanism of CCM pathogenesis. *Hum. Mol. Gen.*, **18**, 919-930.

27 Gault, J., Shenkar, R., Recksiek, P. and Awad, I.A. (2005) Biallelic somatic and germ line CCM1 truncating mutations in a cerebral cavernous malformation lesion. *Stroke*, 872-874.

28 Whitehead, K.J., Plummer, N.W., Adams, J.A., Marchuk, D.A. and Li, D.Y. (2004) Ccm1 is required for arterial morphogenesis: implications for the etiology of human cavernous malformations. *Development*, **131**, 1437-1448.

29 Boulday, G., Rudini, N., Maddaluno, L., Blecon, A., Arnould, M., Gaudric, A., Chapon, F., Adams, R.H., Dejana, E. and Tournier-Lasserve, E. (2011) Developmental timing of CCM2 loss influences cerebral cavernous malformations in mice. *J. Exp. Med.*, **208**, 1835-1847.

30 Plummer, N.W., Gallione, C.J., Srinivasan, S., Zawistowski, J.S., Louis, D.N. and Marchuk, D. A. (2004) Loss of p53 sensitizes mice with a mutation in ccm1 (KRIT1) to development of cerebral vascular malformations. *Am. J. Path*, **165**, 1509-1518.

31 McDonald, D.A., Shenkar, R., Shi, C., Stockon, R.A., Akers, A.L., Kucherlapati, M.H., Kucherlapati, R., Brainer, J., Ginsberg, M.H., Awad, I.A. and Marchuk, D.A. (2011) A novel mouse model of cerebral cavernous malformations based on the two-hit mutation hypothesis recapitulates the human disease. *Hum. Mol. Gen.*, **20**, 211-222.

32 McDonald, D.A., Shi, C., Shenkar, R., Stockton, R.A., Liu, F., Ginsberg, M.H., Marchuk, D.A. and Awad, I.A. (2012) Fasudil decreases lesion burden in a murine model of cerebral cavernous malformation disease. *Stroke*, **43**, 571-574.

CHAPTER 2

LACK OF CCM1 RESULTS IN HYPERSPROUTING AND IMPAIRS RESPONSE TO FLOW

The following chapter was reprinted with permission from the Oxford University Press. In addition to myself, the other authors were Aubrey Chan, Mike Redd, Christopher Gibson, Chadwick Davis, Dallas Shi, Tiehau Chen, Kandis Carter, Jing Ling, Raquel Blanco, Holger Gerhardt, Kevin Whitehead, and Dean Li. It was originally published in Human Molecular Genetics, Epub 2014 Jul 18. I participated in the design, execution, and interpretation of data and in the preparation of the manuscript.

HMG Advance Access published July 18, 2014

Human Molecular Genetics, 2014 ***1–12***
doi:10.1093/hmg/ddu342

Lack of CCM1 induces hypersprouting and impairs response to flow

Tara M. Mleynek[1,2], Aubrey C. Chan[1,2], Michael Redd[3], Christopher C. Gibson[1,5], Chadwick T. Davis[1,4], Dallas S. Shi[1,4], Tiehua Chen[1,6], Kandis L. Carter[1,6], Jing Ling[1], Raquel Blanco[7], Holger Gerhardt[8], Kevin Whitehead[1,6,9] and Dean Y. Li[1,2,9,10,*]

[1]Department of Molecular Medicine, [2]Department of Oncological Sciences, [3]Flourescence Imaging Core, [4]Department of Human Genetics, [5]Department of Bioengineering, [6]Small Animal Ultrasound Core, University of Utah, Salt Lake City 84112, USA, [7]Vascular Biology Laboratory, London Research Institute, Cancer Research UK, London WC2A 3LY, UK, [8]Vascular Patterning Laboratory, VIB3-Vesalius Research Center and CMVB, Department of Oncology, KU Leuven Campus Gasthuisberg O&N4, Herestraat 49 box 912, Leuven B-3000, Belgium, [9]Division of Cardiovascular Medicine, Salt Lake City 84132, USA and [10]The Key Laboratory for Human Disease Gene Study of Sichuan Province, Institute of Laboratory Medicine, Sichuan Academy of Medical Sciences & Sichuan Provincial People's Hospital, Chengdu, Sichuan 610072, China

Received February 14, 2014; Revised June 18, 2014; Accepted June 30, 2014

Cerebral cavernous malformation (CCM) is a disease of vascular malformations known to be caused by mutations in one of three genes: *CCM1*, *CCM2* or *CCM3*. Despite several studies, the mechanism of CCM lesion onset remains unclear. Using a *Ccm1* knockout mouse model, we studied the morphogenesis of early lesion formation in the retina in order to provide insight into potential mechanisms. We demonstrate that lesions develop in a stereotypic location and pattern, preceded by endothelial hypersprouting as confirmed in a zebrafish model of disease. The vascular defects seen with loss of *Ccm1* suggest a defect in endothelial flow response. Taken together, these results suggest new mechanisms of early CCM disease pathogenesis and provide a framework for further study.

INTRODUCTION

Cerebral cavernous malformation (CCM) is a disease characterized by the formation of dilated vascular lesions in the brain, retina and skin (1). CCM lesions lack the typical blood-tight barrier of healthy vessels, resulting in chronic leakiness and associated inflammation in the surrounding tissue and most commonly lead to headaches, seizures and strokes (2). The disease affects as much as 0.5% of the population (1,3,4) and can occur sporadically or be inherited in an autosomal dominant pattern. The inherited form of the disease is caused by the loss of function of one of three genes: *CCM1*, *CCM2* or *CCM3* (5).

Loss of CCM1, encoding the protein Krev-interaction trapped protein-1 (KRIT1), has been shown to disrupt several cellular processes *in vitro* and *in vivo*, including the appropriate organization of the junctional protein VE-Cadherin and endothelial cell polarity (6,7). Maintaining physiologic cell–cell junctions and cell polarity are critical to normal cell migration, flow response and appropriate signaling by various cascades (8). There are many other dysfunctional processes associated with loss of CCM1 *in vitro*, but how these interact *in vivo* to disrupt normal cellular physiology is unknown. Current models and systems have focused on established lesions, but the preceding events that initiate lesion formation have not been identified.

While models are useful for interrogation of the disease, later stage models can mislead when secondary downstream effects are interpreted as primary defects. Understanding the events that lead to interpretable signs of disease provides invaluable insight into the pathophysiology of CCM disease. Therefore we sought to analyze the developmental events that give rise to cerebral cavernous malformations associated with loss of *CCM1* in hopes of identifying a morphological tipping point.

*To whom correspondence should be addressed at: Building 533, Room 4220, 15 N 2030 East, Salt Lake City, UT 84112, USA. Tel: +1 8015855505; Fax: +1 8015850701; Email: dean.li@u2m2.utah.edu (D.Y.L.).; 30 North 1900 East, Room 4A100, Salt Lake City, UT 84132, USA. Tel: +1 8015817715; Fax: +1 8015817735; Email: kevin.whitehead@u2m2.utah.edu (K.J.W.)

The murine embryonic phenotype associated with homozygous deletion of *Ccm1* consists of severe defects of the aorta and branchial arch arteries resulting in death, making the murine embryo a challenging system for studying the onset of CCM lesion formation (9). We therefore created an inducible mouse model of CCM disease where loss of a second CCM allele from the endothelium can be induced after birth in a heterozygous mouse (10,11), allowing normal developmental angiogenesis and vascular patterning to occur and mimicking the loss of heterozygosity thought to predispose to lesion formation. In our model, we find that retinal lesions develop early in life, adhere to a strict stereotypical pattern and form following hypersprouting of the retinal vasculature front. In addition, we find that cells deficient in CCM1 fail to align to flow in an *in vitro* model and that loss of *ccm1* in the zebrafish phenocopies loss of blood flow, suggesting that failed endothelial flow response may be a contributing mechanism for CCM1 lesion development.

RESULTS

Generation of CCM1 mutant alleles

A homozygous germline knockout of *Ccm1* results in vascular tissue defects as early as E8.5, including failure of the branchial arch artery and caudal portion of the dorsal aorta to form a lumen. These defects restrict and disrupt normal blood flow (9). In order to determine whether *Ccm1* is required autonomously in endothelial cells, we created a conditional allele in which exons 4–8 of *Ccm1* were flanked by loxP sites and Cre recombinase was expressed in specific cell types using different tissue-specific Cre drivers (Supplementary Material, Fig. S1). In embryos with a germline mutant *Ccm1* allele and a second floxed allele of *Ccm1*, the endothelial loss of *Ccm1* driven by co-expression of a tissue-specific Cre (Tie2-Cre) (12) resulted in mice with a homozygous deletion of *Ccm1* restricted to the endothelium. With the loss of *Ccm1* in the endothelium, embryos fail to survive beyond E12.5 due to failed vascular development. The branchial arch arteries fail to lumenize properly as seen by immunofluorescent staining of the vasculature (Fig. 1A–F). We examined the effects this impaired lumen formation could have on circulation by performing India ink microangiography, a technique used to assess vessel patency. The disrupted vessel formation prevented normal passage of ink through the branchial arch arteries (Fig. 1G and H). This failure in proper embryonic circulation could also be detected by *in utero* ultrasound (Fig. 1I and J). The development of the impaired lumen organization and failed circulation in the endothelial knockout is similar to that described previously in the germline knockout, a pattern akin to loss of *Ccm2* but not *Ccm3* (10,11).

Having observed that endothelial specific loss of *Ccm1* generates defects that are nearly indistinguishable from the embryonic defects in germline knockouts (9), we inquired if post-natal induction of loss of a second allele of *Ccm1* would produce a murine model that would more closely mimic human disease. Therefore, we utilized an inducible Cre, PDGFb-iCreERT2, the expression of which is also restricted primarily to the endothelium, but is activated only upon exposure to tamoxifen (13). To confirm the endothelial specificity, we crossed the PDGFb-CreERT2 mouse with the mTmG reporter mouse. Following tamoxifen administration the GFP expression was detected in the endothelium as confirmed with a co-stain with the endothelial marker lectin (Supplementary Material, Fig. S2). This system allowed us to knockout the second *Ccm1* allele at any

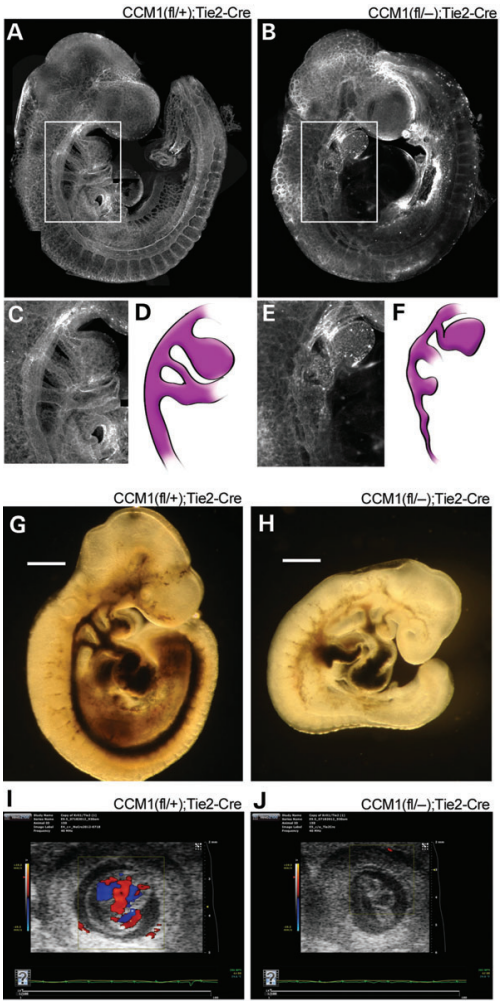

Figure 1. Endothelial loss of CCM1 results in abnormal embryonic vascular development. (**A** and **B**) Visualization of the vasculature, as indicated by lectin stain, or whole-mount embryos at E9.5. (**C** and **E**) Close-up image of the branchial arch artery morphology from the indicated white outlines in A and B. (**D** and **F**) Illustration of the branchial arch artery from the adjacent panel, included to highlight visualization. (**G** and **H**) Brightfield images of ink injected E9.5 embryos. Light blue arrows indicate areas where ink was able to flow through the vasculature. (**I** and **J**) *In utero* ultrasound of blood flow on E9.5 embryos. Embryos are located in the center of each image with the box indicating the area being monitored for flow. The heat map bar on the left indicates the directionality of the blood flow, red indicates blood flow towards the camera, blue indicates blood flow away from the camera. Absence of color demonstrates absence of flow.

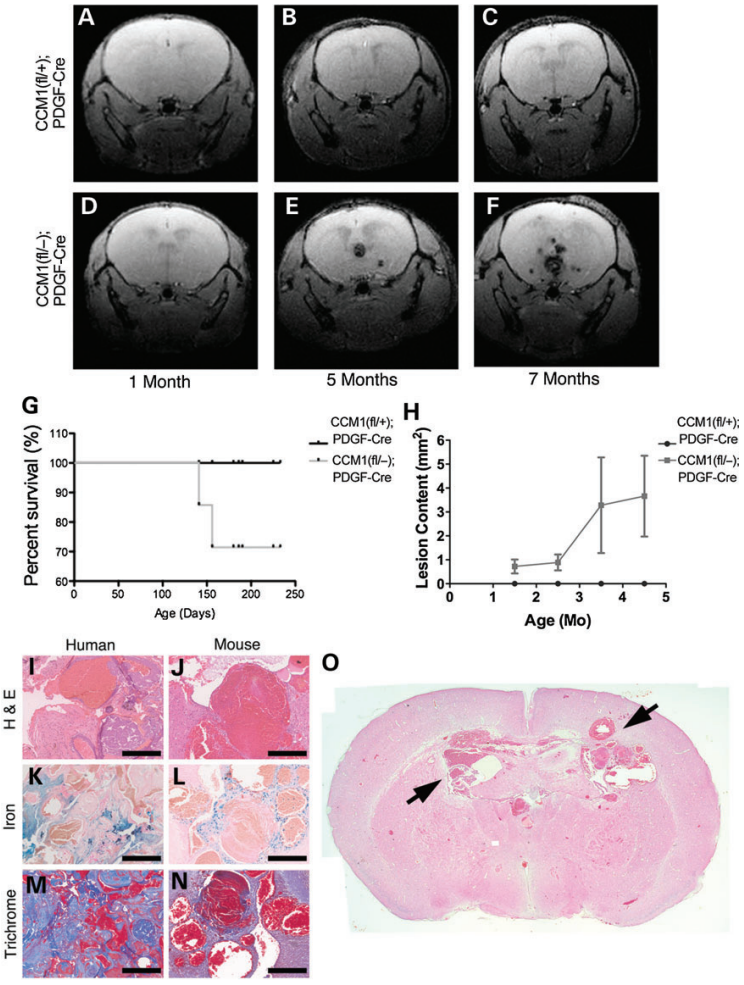

Figure 2. Post-natal endothelial loss of CCM1 phenocopies human disease. (**A**–**F**) Live animal magnetic resonance imaging (MRI) images of mice. Each row is from one mouse, kept alive, and imaged successively over time at the ages indicated in the panel. Light blue arrows indicate CCM lesions. (**G**) Kaplan–Meier survival curve, animals were given tamoxifen at birth and followed through life. Animals that survived were euthanized at 8 months of age. (**H**) Quantification of CCM brain lesion content over time. Lesion burden is determined as the total number of lesions observed in each tomographic view (slice) of the MRI per mouse. (**I**–**N**) Histological staining comparing samples from human CCM1 lesions and lesions from CCM1 knockout mice. H&E staining indicates tissue morphology of the lesion. Iron staining indicates leak into the brain tissue surrounding the lesion. Trichrome staining indicates fibrosis surrounding the lesion. Scale bar at 200 μm. (**O**) Whole-brain H&E histology of an 8-month old CCM1 knockout mouse. Black arrows indicate CCM lesions.

time point after birth, bypassing the lethal embryonic defects. Endothelial specific deletion of the floxed allele can be obtained by crossing the PDGF-iCreERT2 allele into the floxed *Ccm1* background. This allele results in an induced endothelial knockout (ieKO) upon stimulation with tamoxifen. The loss of endothelial *Ccm1* following tamoxifen treatment at birth leads to the formation of cavernous malformations in the brains of all animals. We tracked the development from simple, dilated telangiectasias to large multi-chambered caverns over time using live animal magnetic resonance imaging (MRI). Lesion pathology includes vascular leak, which results in the deposition of hemosiderin which is detected by the MRI and presents as dark masses within the brain. These lesions arise throughout the entire brain by 2 months and progress in severity with time (Fig. 2A–F). The presence of these lesions decreased the survival rate in mice, which correlated with increased lesion content (Fig. 2G and H). Further analysis showed that histologically these lesions phenocopy the hallmarks of human disease with dilated, thin-walled

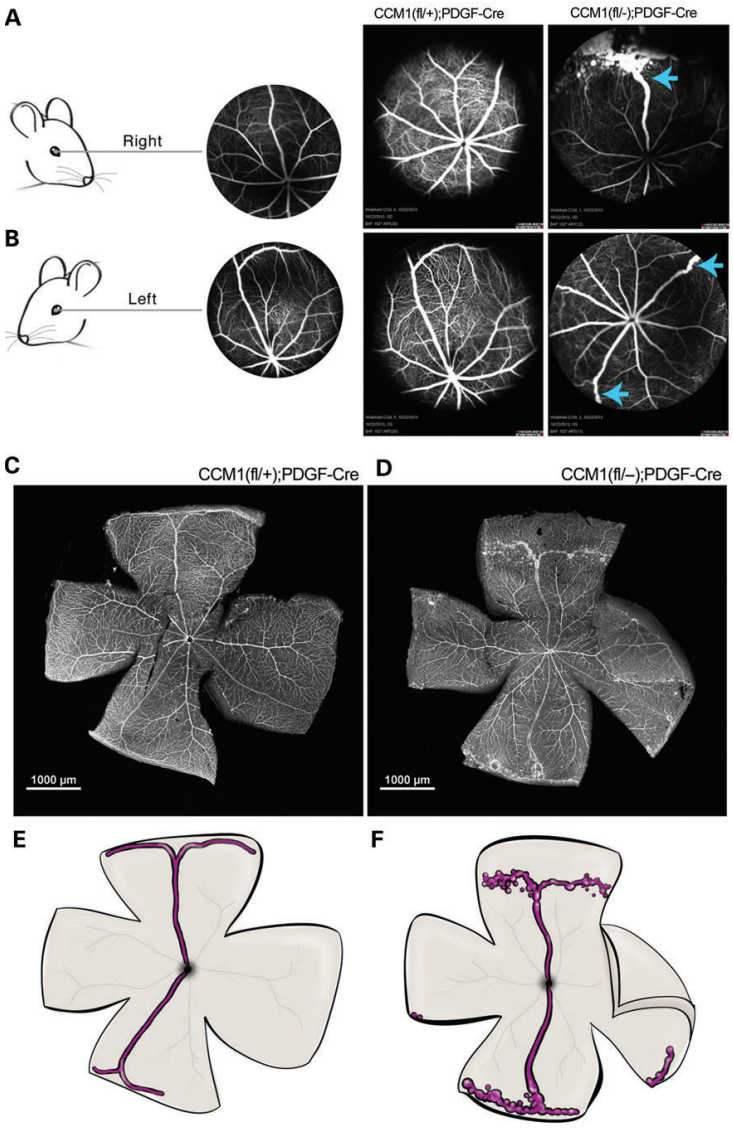

Figure 3. Retinal CCMs develop in a stereotypical location. (**A** and **B**) Schematic indicating mouse retinal orientation, right in A and left in B, with an example angiograph showing the expected retinal vascular morphology. Adjacent to the example angiography are live angiographs taken from either control or CCM1 knockout mouse in the appropriate orientation. Blue arrows indicate lesion location. Scale bars are at 1000 μm. (**C** and **D**) Visualization of retinal vascular, as indicated by lectin staining, in whole-mount retinas from the mice shown in B (left eyes). (**E** and **F**) Schematic illustration highlighting lesion location and morphology. The superior and inferior veins are colored in purple with the major surrounding vessels in light gray.

caverns surrounded by hemosiderin deposits (reflecting ongoing vascular leak), inflammation and fibrosis (Fig. 2I–O) (14). Lesions also consistently form in the retinas of all affected animals (Fig. 3). Because of its size and ease of access, the retina is well characterized with respect to normal vascular development (15) and is thus an ideal focal point for describing the early

developmental mechanism of CCM lesion formation. Moreover, the retina is amenable to live-animal angiography, permitting us to ask questions of lesion perfusion as well as location.

In order to examine the location and perfusion of retinal cavernous malformations, we studied ieKO mice with *in vivo* fluorescein angiography. Using this method, we found that lesions stereotypically arise in the veins located both most superior and inferior within the retina (Fig. 3A and B). Extending out from the trunk of these veins is a tangled network of spherical vascular sacs, the hallmark of cavernous malformation anatomy (16). The individual caverns are confined to the periphery, vary in size and are interconnected by narrow vessels. These vessels also appear to be fully perfused as indicated by the ability of the fluorescein to fill the lesions. Visualization of these retinas via dissection and lectin staining confirmed our observations from the angiography (Fig. 3C–F).

We next examined the timing of lesion formation by looking at a series of retinas from mice at different ages. Retinas from ieKO remain indistinguishable from controls until postnatal Day 7 when the vascular network begins to exhibit vessel dilation and failure of plexus coalescence. Over time, the vascular dilations resolve into caverns and by p21 the lesions assume the well-defined morphology of a mature retinal CCM and recapitulate human retinal angiomas (Fig. 4A–J) (16). We found that this pattern of development held true for 100% of the retinas examined and that all of the *Ccm1* knockouts developed retinal lesions.

The normal growth of retinal vasculature begins at birth with endothelial cells expanding across the superficial layer (17). At P8 the formation of a vascular network in the deep retinal layer begins. Eventually the superficial and deep networks are joined together by the formation of an intermediate network. Once these layers are interconnected and the vascular network has reached the periphery of the retina, angiogenesis is complete and the retinal vasculature is mature. We found that CCM lesions arose from the superficial vascular plexus and remained superficial until later in disease progression. At P10 the dilations observed in early disease onset were limited to the superficial layer with no dilated caverns observed in the deep or intermediate layers (Fig. 4K′–R′). By 5 months the main body of the lesion remained superficial but some extension of caverns could be observed in the deeper layers as the mature lesion expanded in size (Fig. 4K–R). The superficial location of the lesions could also be seen using cross sectional analysis (Fig. 4S–X). To further expand on our observation that lesions were perfusable, we conducted ultrasound studies of the retinal vasculature. We found no difference in blood flow between ieKO and control mice, implying that retinal cavernous malformations are low flow lesions that do not increase the overall retinal blood flow (Fig. 5A–C).

The first 2 weeks of retinal development relies heavily on active angiogenesis, particularly as the superficial plexus expands (18,19). However, by P21, retinal angiogenesis is complete and the vascular structure is mature. To determine if lesion formation was dependent upon this early angiogenic process, we inactivated *Ccm1* at varying time points after birth and followed the subsequent retinal development. We found that when *Ccm1* is lost at the critical point of phenotype distinction, P7, lesions do form in the periphery of the retina by P21 and that these lesions demonstrate similar morphology as those of mice induced at birth, though the severity and size of the lesions are diminished (Fig. 5D and E). If we delay delivery of tamoxifen such that *Ccm1* is not deleted until P21, after the retinal vasculature is mature, we find that lesions do not form (Fig. 5F). Therefore, our results in a distinct animal model confirm those of others that active angiogenesis is required for lesion formation (20).

Lack of CCM1 induces hypersprouting

Sprouting angiogenesis requires the coordinated effort of multiple endothelial cells and is found at the leading edge of the developing vascular plexus (18). It is dictated by the stochastic response of select endothelial cells responding to angiogenic stimuli. The responsive cells that form the sprouts (called tip cells) extend, migrate and fuse to develop a vascular plexus (19). The non-responsive cells that remain non-migratory are known as stalk cells. Therefore, it is possible that excessive sprouting and the subsequent anastomosis could contribute to lesion onset. Prior to vessel dilation, we find that retinas from ieKO mice induced at P1, exhibit endothelial hypersprouting (Fig. 6A–C). The sprouts observed showed a tip cell phenotype as indicated by the tip cell marker PDGFb as well as cellular morphology (Supplementary Material, Fig. S2). Although the retina allows better observation of the three-dimensional architecture of the cavernous malformation than the mouse brain, it is difficult to observe the dynamics of vascular development in the intact mouse eye in real time. Sprouting angiogenesis is a dynamic process, therefore we sought to explore this phenotype in a model more amenable to live imaging. Zebrafish have the advantage of *ex vivo* development and transparency that allow the real-time observation of sprouting angiogenesis. (21). Therefore, we sought to evaluate sprouting angiogenesis in a zebrafish model.

To examine early angiogenic sprouting, we injected a morpholino targeted against *ccm1* (22) (or a scrambled control) at the single cell stage of embryos carrying the endothelial specific reporter kdrl;GFP. We found that the caudal vein plexus (CVP) development exhibited hypersprouting at 28 h post-fertilization (hpf) (Fig. 6D and E) and then went on to develop into a large vascular cavern, a defect similar to early retinal lesions (Fig. 6F–K). The dilation of the CVP is also reminiscent of the dilated caudal dorsal aorta in developing CCM1 knockout mouse embryos, which also demonstrated alterations in artery/vein specification. Loss of this morphological distinction between the caudal artery and the cadual vein in the zebrafish and the resulting dilated morphology, highlights overlap in the vascular pathology of both mouse and zebrafish. Under normal developmental circumstances the CVP arises from the process of ventral sprouting. Ventral sprouting initiates at 20 hpf when endothelial cells begins to sprout and migrate from the dorsal aorta (23). The cells then expand as a population and coalesce into the distinct vascular network of the CVP (Supplementary Material, Movie S1). In contrast, when *ccm1* is reduced, the cells do not form a distinct vascular network and the CVP develops as a large vascular sac (Supplementary Material, Movie S2). Therefore these data suggest that the formation of CCMs could arise from a defect of population-wide endothelial hypersprouting and anastomosis, resulting in a malformed vascular cavern.

Lack of CCM1 impairs flow response

Flow can regulate vascular morphology during development (24) and shear stress can direct overall network architecture.

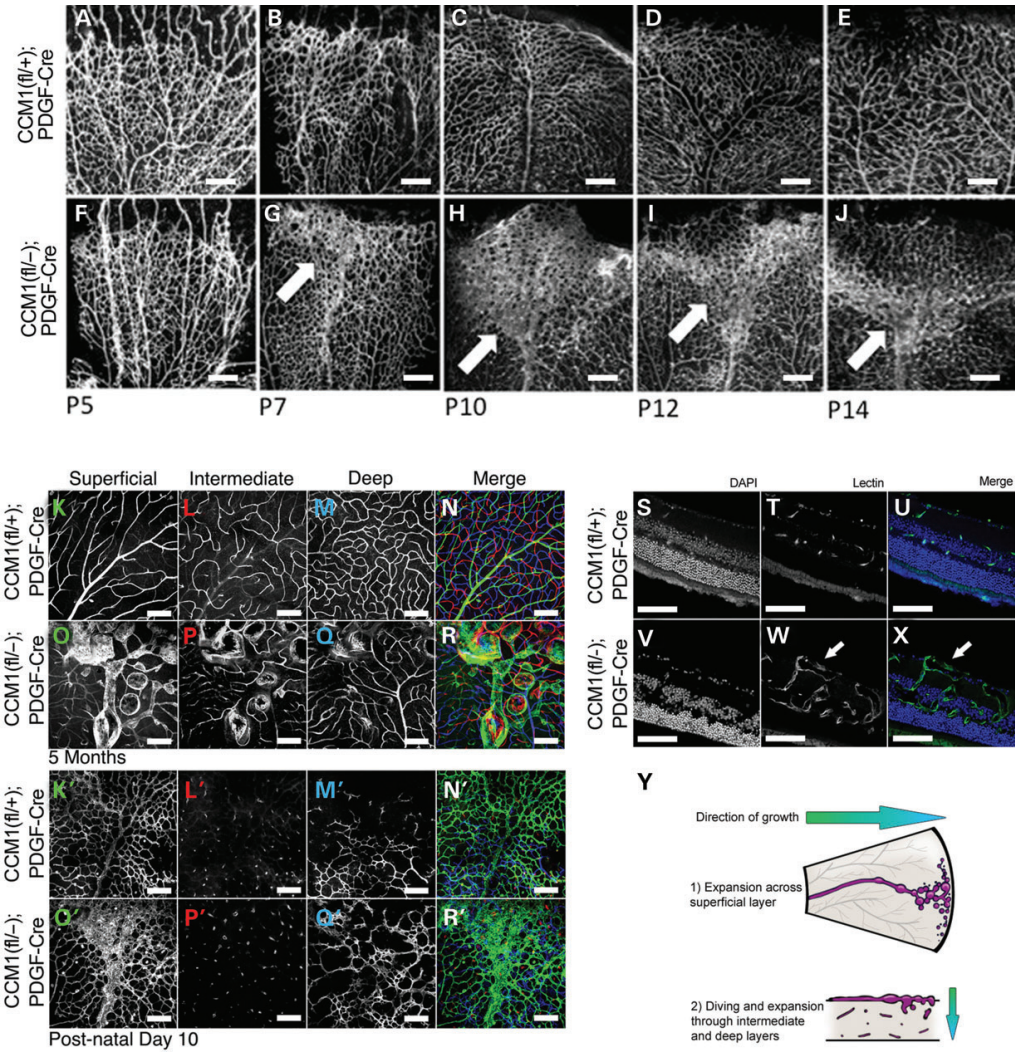

Figure 4. Retinal CCMs develop early and are limited to the superficial vascular plexus. (**A**–**J**) Timecourse of retinal vascular development in denoted genotypes. Retinas were dissected at the ages indicated, then lectin stained and imaged. Each image depicts a single leaflet of the dissected retina. Light blue arrows indicate the location of lesion development. Scale bars = 200 um. (**K**–**R**) Retinal depth images taken at 5 months of age from either a control or CCM1 knockout mouse. Each image was taken using confocal microscopy with the microscope focused in the retinal plane indicated in the panel (N,R represent merged image. Blue = deep layer. Red = intermediate layer. Green = superficial layer). K′–R′) Retinal depth images taken at 10 days of age from either a control or CCM1 knockout mouse. Each image was taken using confocal microscopy with the microscope focused in the retinal plane indicated in the panel (N,R represent merged image. Blue = deep layer. Red = intermediate layer. Green = superficial layer). (**S**–**X**) Cross sectional images from 5-month-old retinas from either control or CCM1 knockout mice. Each retina was frozen in OCT, sectioned and stained with lectin and DAPI to visualize both the vasculature and the surrounding tissue. (**Y**) Diagram depicting lesion growth across the retina. All scale bars set at 200 μm.

Furthermore blood flow can attenuate endothelial sprouting (25). The effects of flow and the endothelial mechanism to detect flow may provide an explanation for the hypersprouting observed as well as why lesions form stereotypically.

The silent heart morpholino, which knocks down cardiac troponin, results in a non-beating heart resulting in a complete lack of blood flow (26). We find that at 28 hpf silent heart morphants exhibit the same hypersprouting defect as seen in the

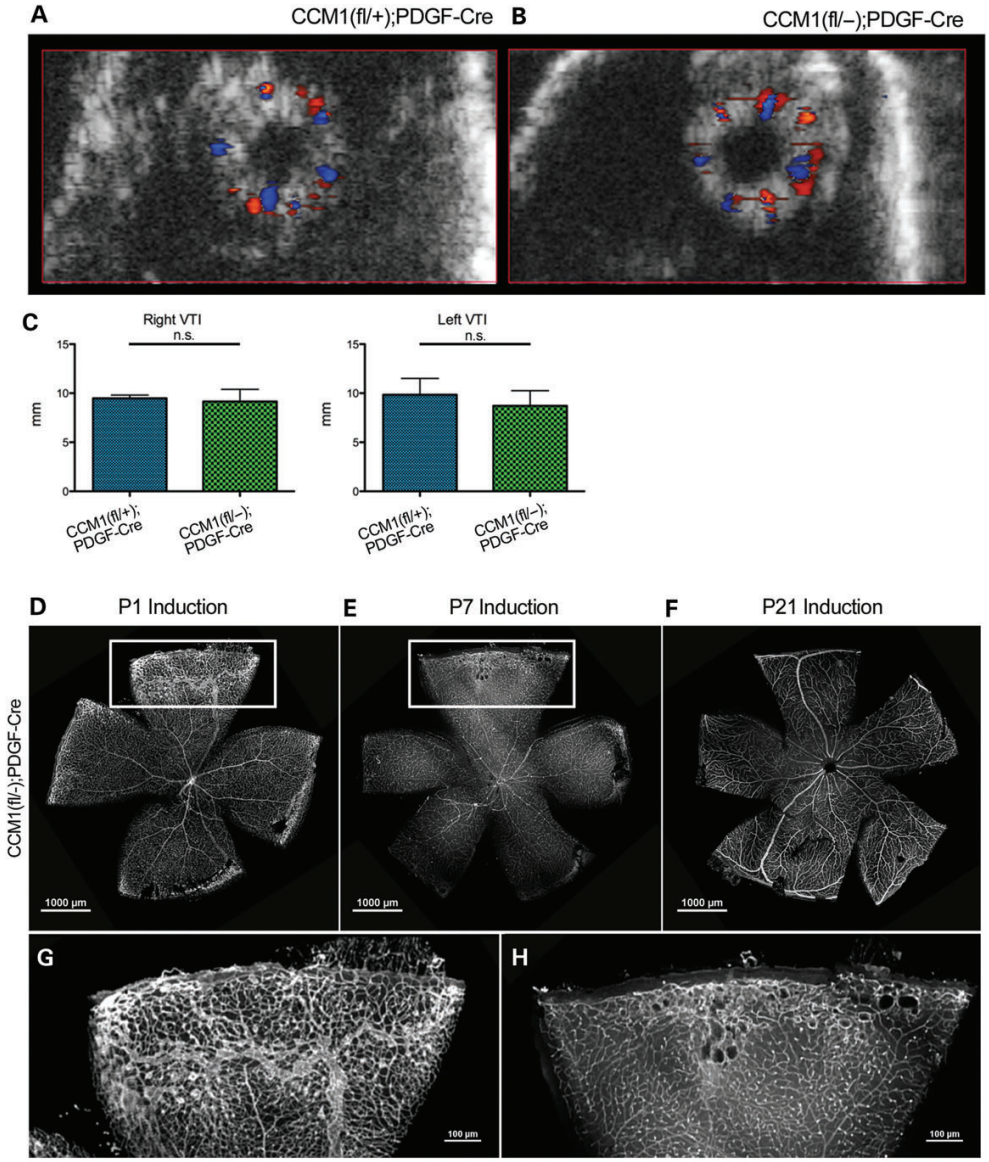

Figure 5. Retinal CCMs do not exhibit disrupted hemodynamics and are limited to a specific developmental window. (**A** and **B**) Ultrasound images of whole retinal vasculature from either control or knockout mice, orientation is en face with the optic nerve in the center of the eye. Red color indicates blood flow towards the camera, blue color indicates blood flow away from the camera. (**C**) Quantification of the volume time interval (VTI) of both left and right eyes as calculated by the Vevo2100 software. (**D**–**F**) Visualization of the retinal vasculature, as indicated by lectin stain, from a CCM1 knockout mouse that was induced at P1 (D imaged at P21), induced at P7 (E imaged at P21) or induced P21 (F imaged at 8 months). (**G** and **H**) Close-up of the vascular lesion from the insets in E and F. Scale bars set at 1000 µm.

ccm1 morphants. In addition, the silent heart morphants go on to develop the CVP dilation as seen in the ccm1 morphants (Fig. 7A–G, Supplementary Material, Movie S3). However, flow is present in 37% of the *ccm1* morphants and yet these morphants still develop the same defects (Supplementary Material, Movies S4 and S5), suggesting defects in blood flow or

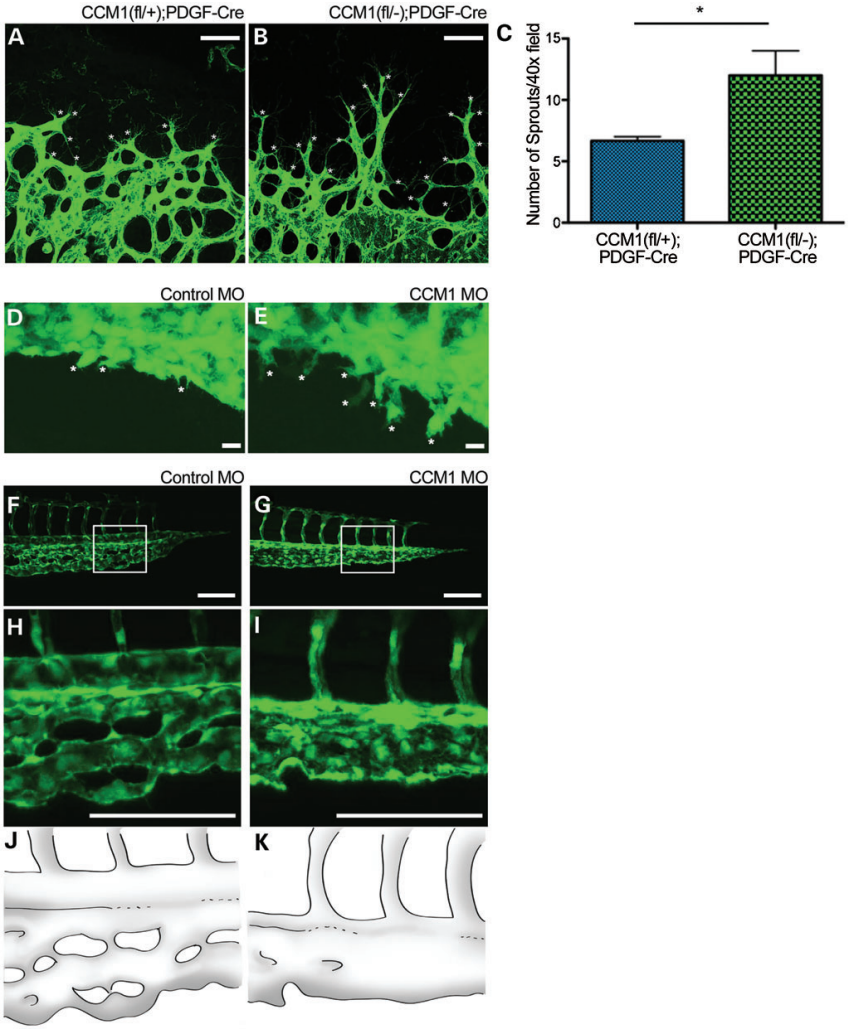

Figure 6. Loss of CCM results in hypersprouting. (**A** and **B**) Images showing sprouting at the retinal vascular front at Day p7 as indicated by lectin stain. White asterisks denote sprouts. Scale bars set at 50 μm. (**C**) Quantification of sprouts per field at p7, *P*-value <0.05. (**D** and **E**) Endothelial sprouting of the zebrafish CVP at 28hpf. White asterisks denote sprouts. Scale bars set at 100 μm. (**F** and **G**) Zebrafish tail vasculature at 48 hpf. White box indicates area of inset. (**H** and **I**) Inset of tail vasculature. (**J** and **K**) Schematic illustration highlighting the tail morphology seen in F and G.

the ability to sense blood flow might be contributing to lesion formation.

We therefore hypothesized that *CCM1* is required for the endothelial cell to sense or respond to flow. We predicted that cells deficient in *CCM1* would exhibit hallmark defects, such as an inability to align to the direction of flow (27). To test endothelial response to shear stress, we suppressed *CCM1* expression in monolayers of HUVEC cells using siRNA. These monolayers were then exposed to a period of laminar shear stress and their alignment was analyzed by measuring the major angle of an ellipse fitted to each cell in relation to the direction of flow. Cells depleted of *CCM1* failed to align with the direction of blood flow, consistent with a role for flow in the formation of CCM lesions (Fig. 7H–L).

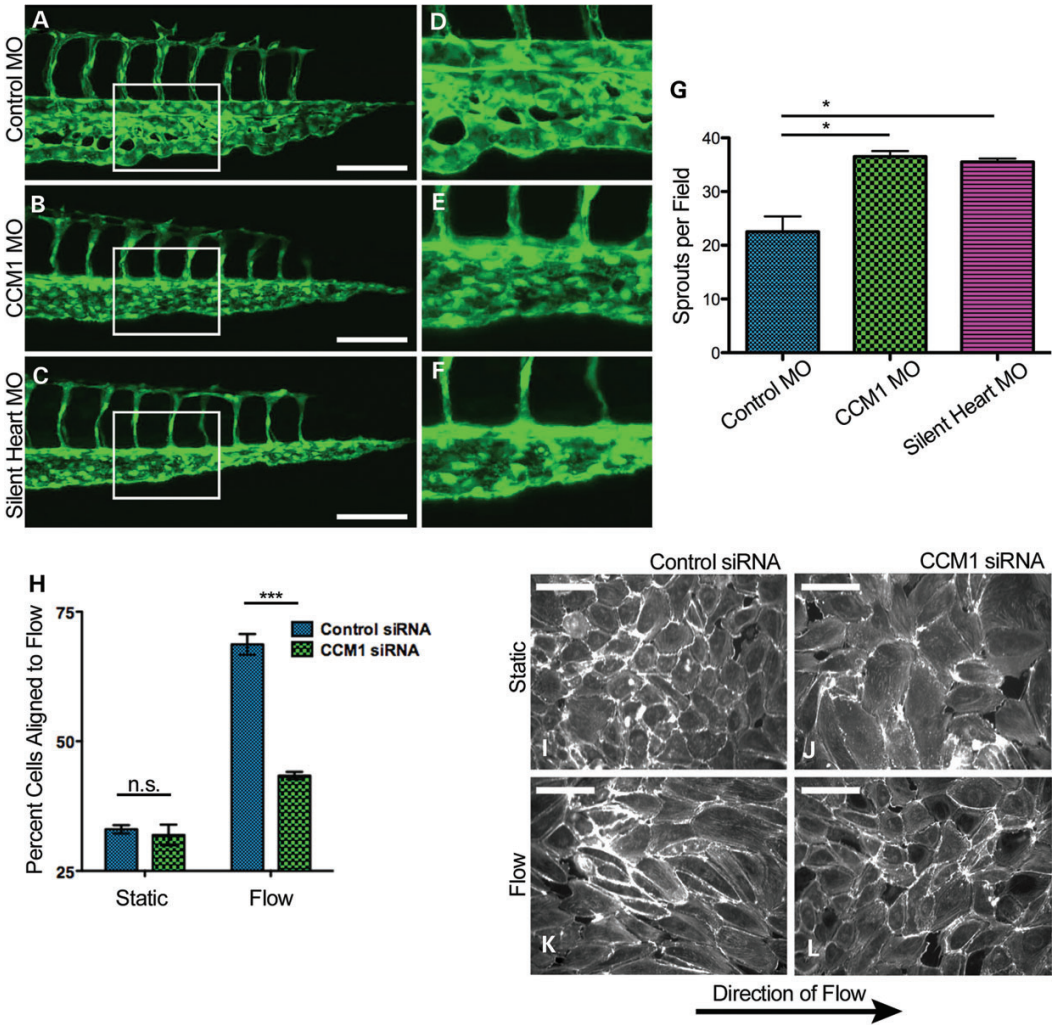

Figure 7. Loss of CCM results in impaired flow response. (**A**–**C**) Images of zebrafish tail morphology at 48 hpf. White box indicates area of inset. (**D**–**F**) Inset of tail vasculature. (**G**) Quantification of endothelial CVP sprouting at 28 hpf. *P*-value <0.05. (**H**) Quantification of I-L, *P*-value <0.0001. (**I**–**L**) Endothelial monolayers stained with phalloidin and exposed to either static (**F** and **G**) or flow (**H** and **I**) conditions. Scale bars at 40 μm.

DISCUSSION

The current field of CCM study has focused primarily on late-stage disease, with read-outs being in mature disease states. Such an approach is limited in scope and can overlook the stimulus that initiates lesion formation. Understanding the developmental process of CCM formation is critical in identifying the key molecular events that lead to disease onset. By taking a developmental approach, our study represents a careful analysis of the early morphological events of CCM formation. We demonstrate that retinal lesions develop in a stereotypic pattern and location. In addition, we find that *Ccm1* must be lost during a particular developmental window in order for lesions to form, consistent with the observations of Boulday *et al*. (20). Furthermore, we find that prior to any sort of vascular dilation phenotype endothelial cells exhibit a hypersprouting behavior. Hypersprouting in conjunction with the predictable development of the lesions from veins suggests that local cues may be a contributing factor to disease onset.

Previous work demonstrating that blood flow can regulate sprouting and organization suggested a potential mechanism

for the development of CCM lesions. The difference in arterial and venous flow rates provides local developmental cues to endothelial cells via the process of flow response (24). A defect in flow response could explain why lesions develop in a stereotypic pattern and are restricted to the superior and inferior veins. Our observation that endothelial cells deficient in CCM1 do not align to flow and the ability of silent heart to phenocopy the sprouting and dilation phenotype seen with *ccm1* knockdown support the hypothesis that response to flow may be disrupted. In addition, in a previous work by Hogan *et al*. (28) it was observed *in vivo* that loss of CCM1 results in a round cell shape that does not elongate in the direction of flow. This observation is consistent with our finding of failed alignment *in vitro*. If endothelial cells cannot sense or respond to the local flow appropriately, development of the local vascular architecture could be disrupted. Further study is needed in order to determine whether the defect is in sensing flow or in response to flow and how those processes may influence the development of the local vasculature. Taken together, our data demonstrate the predictable nature of retinal CCMs and provide a new approach to the study of this disease. Furthermore, our results illustrate the importance of both the physiology and environment in the etiology of vascular disease.

MATERIALS AND METHODS

Mice

Animals were housed at the University of Utah and all experiments were approved by the University of Utah Institutional Animal Care and Use Committee. The *Ccm1* floxed allele was generated by inserting LoxP sites that flank exons 4–8 (Krit1^{tm1Kwhi}, here referred to as *Ccm1*^{flox}). A germline mutant allele (*Krit1*$^{tm1.1Kwhi}$, here referred to as *Ccm1*-) was generated by crossing these mice against mice expressing Cre recombinase in the germline. See Supplementary Material, Figure S1. The mT/mG (B6.129 (Cg)-Gt (ROSA)26Sor$^{tm4(ACTB-tdTomato,-EGFP)Luo}$/J) was obtained from Jackson Labs.

Human samples

Human tissue samples were provided by Connie Lee and Amy Akers (Angioma Alliance, Norfolk, VA, USA) and Randy Jensen (University of Utah, Salt Lake City, UT, USA) and were obtained with written informed consent. Human experiments were approved by the Institutional Review Board of the University of Utah.

Zebrafish

Zebrafish were maintained under standard husbandry conditions in the University of Utah CZAR and were approved by IACUC. The transgenic lines used were Tg (kdrl:GFP) for endothelial visualization and Tg (gata1:dsRed) for red blood cell visualization. Morpholino injections were done using standard injection techniques and the previously described morpholinos for CCM1 (22) and Silent Heart (26).

Analysis of mouse embyos

Embryos were harvested at time indicated and confocal immunofluorescence or fetal ultrasound was performed as previously described (11). Ink injections were done as previously described (29)

MRI

MRI studies were conducted as previously described (10)

Antibodies

For endothelial visualization in retina immunofluorescence Alexa Fluor Isolectin GS-IB4 (Invitrogen) was used. For actin visualization Alexa Fluor phalloidin (Invitrogen) was used.

Histology

Adult mouse brains were removed after fixation in 4% formaldehyde for at least 3 days or zinc-buffered formalin overnight. The brain was then removed and sliced into three coronal sections and was embedded into paraffin by standard protocol. Histological staining for iron and trichrome were carried out using the Dako Artisan system according to manufacturer's instructions.

Microscopy

All fluorescent still images were taken using the Nikon AR1 confocal microscope using either a $\times 10$, $\times 20$ or $\times 40$ objective. For live zebrafish imaging, the Nikon Eclipse Ti widefield was used in conjunction with temperature controlled stage. Fish were mounted in 1% low-melt agarose on a glass cover slip. The coverslips were mounted onto the stage and E3 solution was used to prevent the agarose from drying. Temperature in the imaging chamber was set to 30°C. For brightfield histological imaging, the Zeiss Axioplan 2 microscope was used with either the $\times 10$ or $\times 4$ objective. For the whole-brain histology image (Fig. 2O) several individual panels were taken and then photo-merged into one single image.

Live animal angiography

Prior to anesthesia, 1% Tropicamide was administered to animals to facilitate eye dilation. Animals were then anesthetized using isoflurane, injected with 100 μl of fluorescein, and positioned on the imaging platform. Images were then taken using the Heidelberg SPECTRALIS Ultra-Widefield Angiography Module with the 102° lens while animals were held in consistent orientation.

Retinal processing

Eyes were enucleated and fixed overnight in 4% Paraformaldehyde (PFA) at 4°C. Retinas were then dissected and stained as previously described (19). After staining, retinas were placed into phosphate buffered saline (PBS), cut four times to section the cup into leaflets, and then flat-mounted onto slides using Dako Faramount Aqueous mounting media. For cross-sectional

analysis, eyes were embedded into OCT for frozen sectioning per standard protocol. Sections were cut at 10 μm thickness and then stained with both lectin and DAPI, then mounted with Dako Faramount Aqueous mounting media for imaging.

Fluorescence *in situ* hybridization

Eyes were collected at Day 5 (P5), fixed with 4% PFA 4H and immediately dissected. Retinas were fixed ON with 4% PFA at 4C and transferred to METOH the day after and stored at −80°C Retinas were rehydrated by thorough washing steps with 75, 50 and 25% METOH–PBS–0.1%Tween at RT. Then retinas were treated with Proteinase K (Invitrogen 20 mg/ml. Cat. no. 25530-049) during 20 min, fixed with 4%PFA-0.1% Glutaraldehyde (Sigma, 25% glutaraldehyde solution. Cat. no. G5882) and pre-hybridize at 65°C during 2H with Hb4 hybridization buffer. Probe-hybridization was performed ON at 65°C using Hb4D5 buffer. Hybridization mix was prepared using the digoxigenin (DIG)-probe at concentration of 1 μg/ml. The day after, retinas were thorough washing steps using 50% formamide deionized (Sigma. Cat. no. F9037)-2XSSCT, 2XSSCT and 0.2XSSCT at 65°C, cool down on PBS–0.1%Tween and blocked with PBS–0.1%Tween–8%Sheep serum (Sigma. Cat. no. S2263) during 2H at RT. After that, retinas were incubated ON at 4°C with the sheep anti-DIG peroxidase (POD) antibody (1:500; Anti-DIG-POD Fab fragments. Roche. Cat. no. 11207733910). Next day, retinas were washed during 2H at intervals of 30 min with TBS–0.1%Tween and incubated during 20–30 min with fluorescein tyramide solution (TSA) diluted (1:500) on PBS–0.1%Tween, at RT. For TSA solution synthesis check the link, http://www.xenbase.org/xenwiki/index.php/Flourescin_Tyramide_Synthesis.

Posteriorly, 0.001% H_2O_2 was added to the TSA solution to activate TSA reaction. After 30–45 min TSA reaction was stopped washing quickly the retinas with PBS several times. Before proceeding with Isolectin IF, retinas were washed during 2 day at 4°C in slow agitation with PBS–0.1%Tween to reduce ISH unspecific signal and post-fixed with 4%PFA.

Ultrasound studies of the Eye

Mice were anesthetized with 1.5% isoflurane inhalational anesthetic and monitored for pulse and respiration. Images were acquired from the eye, including specific studies of the retinal artery and vein with B-mode, color and pulsed-wave Doppler modes using a Vevo 2100 high frequency ultrasound machine (VisualSonics).

Cell culture and flow

Human umbilical vein endothelial cells were obtained from Lonza and grown according to the manufacturer's instructions. Human CCM1 or non-targeting siRNA was obtained from Dharmacon. EC transfection with siRNAs was carried out in growth media with 1% serum with details of the siRNA transfection protocol as previously described (30). For flow experiments, cells were plated in IBIDI 8-well chamber slides (VI0.4) and exposed to a 16 dynes/cm^2 flow rate (simulating arterial shear stress) or static conditions for 24 h. Cells were then fixed with 4% PFA and actin cytoskeleton was visualized using phalloidin.

Statistical analysis

For CCM penetrance and lesion content, we performed a two-tailed *t*-test. For quantification of sprouting, we performed a 2-tailed t-test. For analysis of cell alignment, we performed a two-way analysis of variance test. *P*-values are as indicated in the figure legends.

SUPPLEMENTARY MATERIAL

Supplementary Material is available at *HMG* online.

ACKNOWLEDGEMENTS

We would like to thank Brent Bisgrove for the zebrafish Tg (kdrl:GFP) line; O. Abdullah and E. Hsu and the University of Utah Small Animal Imaging Facility; Christopher Rodesch, Mike Bridge and the University of Utah Cell Imaging/Fluorescence Facility; and Sheryl Tripp and the Immunohistochemistry Research and Development Lab at ARUP Laboratories. This work was further supported by the Small Animal Ultrasound core laboratory at the University of Utah. We would also like to thank Kirk Thomas, Shannon Odelberg and Chadwick Davis for their advice, discussions and contributions to the manuscript.

Conflict of Interest statement. None declared.

FUNDING

This work was supported by NIH/NHLBI (grant R01HL065648).

REFERENCES

1. Otten, P., Pizzolato, G.P., Rilliet, B. and Berney, J. (1989) A Study of 131 Cases of Cavernomas of the Cns, discovered on Retrospective Analysis of 24,535 Autopsies. *Neurochirurgie*, **35**, 82–83.
2. Clatterbuck, R., Eberhart, C., Crain, B. and Rigamonti, D. (2001) Ultrastructural and immunocytochemical evidence that an incompetent blood–brain barrier is related to the pathophysiology of cavernous malformations. *J. Neurol. Neurosurg. Psychiatry*, **71**, 188–192.
3. Robinson, J.R., Awad, I.A. and L1ti'le, J.R. (1991) Natural history of the cavernous angioma. *J. Neurosurg.*, **75**, 5.
4. Vernooij, M.W., Arfan Ikram, M., Tanghe, H.L., Vincent, A.J.P.E., Hofman, A., Krestin, G.P., Niessen, W.J., Breteler, M.M.B. and van der Lugt, A. (2007) Incidental findings on brain MRI in the general population. *N. Engl. J. Med.*, **357**, 7.
5. Plummer, N.W., Zawistowski, J.S. and Marchuk, D.A. (2005) Genetics of cerebral cavernous malformations. *Curr. Neurol. Neurosci. Rep.*, **5**, 5.
6. Lampugnani, M.G., Orsenigo, F., Rudini, N., Maddaluno, L., Boulday, G., Chapon, F. and Dejana, E. (2010) CCM1 regulates vascular-lumen organization by inducing endothelial polarity. *J. Cell Sci.*, **123**, 1073–1080.
7. Glading, A., Han, J., Stockton, R.A. and Ginsberg, M.H. (2007) KRIT-1/CCM1 is a Rap1 effector that regulates endothelial cell cell junctions. J. Cell Biol., **179**, 247–254.
8. Lamalice, L., Le Boeuf, F. and Huot, J. (2007) Endothelial cell migration during angiogenesis. *Circ. Res.*, **100**, 782–794.
9. Whitehead, K.J., Plummer, N.W., Adams, J.A., Marchuk, D.A. and Li, D.Y. (2004) Ccm1 is required for arterial morphogenesis: implications for the etiology of human cavernous malformations. *Development*, **131**, 1437–1448.
10. Chan, A.C., Drakos, S.G., Ruiz, O.E., Smith, A.C.H., Gibson, C.C., Ling, J., Passi, S.F., Stratman, A.N., Sacharidou, A., Patricia Revelo, M. *et al.* (2011) Mutations in 2 distinct genetic pathways result in cerebral cavernous malformations in mice. *J. Clin. Invest.*, **122**, 5.

11. Whitehead, K.J., Chan, A.C., Navankasattusas, S., Koh, W., London, N.R., Ling, J., Mayo, A.H., Drakos, S.G., Jones, C.A., Zhu, W. *et al.* (2009) The cerebral cavernous malformation signaling pathway promotes vascular integrity via Rho GTPases. *Nat. Med.*, **15**, 177–184.
12. Kisanuki, Y.Y., Hammer, R.E., Miyazaki, J., Williams, S.C., Richardson, J.A. and Yanagisawa, M. (2001) Tie2-Cre transgenic mice: a new model for endothelial cell-lineage analysis in vivo. *Dev. Biol.*, **230**, 230–242.
13. Claxton, S., Kostourou, V., Jadeja, S., Chambon, P., Hodivala-Dilke, K. and Fruttiger, M. (2007) Efficient, inducible Cre-Recombinase activation in vascular endothelium. *Genesis*, **46**, 6.
14. Liu, H., Rigamonti, D., Badr, A. and Zhang, J. (2010) Ccm1 assures microvascular integrity during angiogenesis. *Transl. Stroke Res.*, **1**, 146–153.
15. Stahl, A., Connor, K.M., Sapieha, P., Chen, J., Dennison, R.J., Krah, N.M., Seaward, M.R., Willett, K.L., Aderman, C.M., Guerin, K.I. *et al.* (2010) The mouse retina as an angiogenesis model. *Invest. Ophthal. Vis. Sci.*, **51**, 2813–2826.
16. Labauge, P., Denier, C., Bergametti, F. and Tournier-Lasserve, E. (2007) Genetics of cavernous angiomas. *Lancet Neurol.*, **6**, 237–244.
17. Dorrell, M.I. and Friedlander, M. (2006) Mechanisms of endothelial cell guidance and vascular patterning in the developing mouse retina. *Prog. Retin Eye Res*, **25**, 277–295.
18. Bentley, K., Mariggi, G., Gerhardt, H. and Bates, P.A. (2009) Tipping the balance: robustness of tip cell selection, migration and fusion in angiogenesis. *PLoS Comput. Biol.*, **5**, e1000549.
19. Gerhardt, H., Golding, M., Fruttiger, M., Ruhrberg, C., Lundkvist, A., Abramsson, A., Jeltsch, M., Mitchell, C., Alitalo, K., Shima, D. *et al.* (2003) VEGF guides angiogenic sprouting utilizing endothelial tip cell filopodia. *J. Cell. Biol.*, **161**, 1163–1177.
20. Boulday, G., Rudini, N., Maddaluno, L., Blecon, A., Arnould, M., Gaudric, A., Chapon, F., Adams, R.H., Dejana, E. and Tournier-Lasserve, E. (2011) Developmental timing of CCM2 loss influences cerebral cavernous malformations in mice. *J. Exp. Med.*, **208**, 1835–1847.
21. Gore, A.V., Monzo, K., Cha, Y.R., Pan, W. and Weinstein, B.M. (2012) Vascular development in the Zebrafish. *Cold Spring Harb.Perspect. Med.*, **2**, a006684.
22. Mably, J.D., Chuang, L.P., Serluca, F.C., Mohideen, M.A., Chen, J.N. and Fishman, M.C. (2006) Santa and valentine pattern concentric growth of cardiac myocardium in the zebrafish. *Development*, **133**, 3139–3146.
23. Herbert, S.P., Huisken, J., Kim, T.N., Feldman, M.E., Houseman, B.T., Wang, R.A., Shokat, K.M. and Stainier, D.Y. (2009) Arterial-venous segregation by selective cell sprouting: an alternative mode of blood vessel formation. *Science*, **326**, 294–298.
24. le Noble, F., Fleury, V., Pries, A., Corvol, P., Eichmann, A. and Reneman, R.S. (2005) Control of arterial branching morphogenesis in embryogenesis: go with the flow. *Cardiovasc. Res.*, **65**, 619–628.
25. Munn, J.W.S. and Munn, L.L. (2011) Fluid forces control endothelial sprouting. *Proc. Natl. Acad. Sci. U. S. A.*, **108**, 5.
26. Sehnert, A.J., Huq, A., Weinstein, B.M., Walker, C., Fishman, M. and Stainier, D.Y. (2002) Cardiac troponin T is essential in sarcomere assembly and cardiac contractility. *Nat. Genet.*, **31**, 106–110.
27. Li, Y.S., Haga, J.H. and Chien, S. (2005) Molecular basis of the effects of shear stress on vascular endothelial cells. *J. Biomech.*, **38**, 1949–1971.
28. Hogan, B.M., Bussmann, J., Wolburg, H. and Schulte-Merker, S. (2008) ccm1 cell autonomously regulates endothelial cellular morphogenesis and vascular tubulogenesis in zebrafish. *Hum. Mol. Genet.*, **17**, 2424–2432.
29. Urness, L.D., Sorensen, L.K. and Li, D.Y. (2000) Arteriovenous malformations in mice lacking activin receptor-like kinase-1. *Nat. Genet.*, **26**, 3.
30. Saunders, W.B., Bayless, K.J. and Davis, G.E. (2005) MMP-1 activation by serine proteases and MMP-10 induces human capillary tubular network collapse and regression in 3D collagen matrices. *J. Cell Sci.*, **118**, 2325–2340.

CHAPTER 3

ENVIRONMENTAL AND GENETIC FACTORS ARE SYNERGISTIC IN THE FORMATION OF CAVERNOUS MALFORMATIONS

In addition to myself contributing authors include Kevin J Whitehead, Hau Su, Aubrey C Chan, Tiehau Chen, Fanxia Shen, Lindan Jiang, Jing Ling, Kandis L Carter, Stavros G Drakos, William L Young, and Dean Y Li. I participated in conducting mouse experiments and manuscript preparation.

3.1 Authors

Title: Environmental and genetic factors are synergistic in the formation of cavernous malformations

Authors: Kevin J. Whitehead[1,2,4,8], Hua Su[5,8], Tara M. Mleynek[1], Aubrey C. Chan[1], Tiehua Chen[1], Fanxia Shen[5], Lidan Jiang[5], Jing Ling[1], Kandis L. Carter[1], Stavros G. Drakos[1,2], William L. Young[5,6,7,9], Dean Y. Li[1,2,3,4]

Author Affiliations:
The Program in Molecular Medicine[1], and the Division of Cardiovascular Medicine[2], and the Division of Oncological Sciences[3], University of Utah, Salt Lake City, UT
George E. Wahlen Department of Veterans Affairs Medical Center[4], Salt Lake City, UT
Department of Anesthesia and Perioperative Care, Center for Cerebrovascular Research[5], and Departments of Neurological Surgery[6] and Neurology[7], University of California San Francisco, San Francisco, CA

These authors contributed equally to this report[8]

Deceased[9]

3.2 Abstract

Cerebral cavernous malformations (CCM) are common vascular lesions are of the central nervous system that occur in both sporadic and familial forms. Evidence is gathering that the loss of both alleles for any of three disease-associated genes underlies both familial and sporadic disease through a so-called “two hit model” analogous to Knudson’s classic description for retinoblastoma. Using an animal model of the most severe and susceptible form of familial disease, Ccm3, we show that delaying the timing of the second genetic hit by 3 weeks completely eliminates disease susceptibility. Our data suggest genetic factors are sufficient to cause CCM lesions only if they occur early in life, calling the universal applicability of the two genetic hit model into question. Using viral vectors to deliver a genetic insult, a local cytokine insult, or both to adult

mice, we show that lesions in adult mice form only in the presence of both genetic and environmental triggers. These data allow the prevailing genetic model for CCM disease to explain the lifelong propensity to form new lesions by demonstrating the synergistic importance of the environmental context.

3.3 Introduction

Cerebral cavernous malformations (CCM) are relatively common vascular malformations of the central nervous system with considerable morbidity. These dilated, thin-walled vessels are prone to vascular leak and rupture and are a significant cause of hemorrhagic stroke (33, 34). They are found with a prevalence of 1 in 200 persons (35-37), and occur in both sporadic and familial forms. For both forms of the disease, the factors associated with lesion formation are incompletely understood. Familial forms have allowed the identification of three genes that are associated with CCM, including CCM1 encoding KRIT1 (38-40), CCM2 encoding OSM/Malcavernin (41-43), and CCM3 encoding PDCD10 (44). Loss of function alleles in any of these three genes afflicts heterozygous carriers with CCM and leads to a more severe form of CCM than sporadic disease characterized by a tendency to form multiple lesions and higher likelihood of symptoms. The earlier onset of symptoms and multiple lesions in heterozygous individuals have suggested the possibility of a “two-hit” genetic mechanism originally suggested by Knudson to explain the development of retinoblastoma (45). Case reports have identified biallelic mutations, one somatic and one germline, for each of the three CCM genes in surgically excised lesions (46-49). Our laboratory and others have shown that the perinatal inactivation of both copies of the CCM genes in the endothelium

of mice is sufficient to induce cavernous malformations in the central nervous system (29, 50). Two genetic "hits" in the first week of life were shown to be sufficient to induce disease in mice.

The compelling evidence supporting the genetic basis of disease has nearly silenced earlier lines of inquiry into environmental causes for CCM. Yet observational data provide reason to believe that environmental factors also influence the formation and progression of CCM disease. Case reports have demonstrated an association between progressive lesion development and elevated serum levels of cytokines, including vascular endothelial growth factor (51, 52). The brain is predisposed to respond with increased cytokine levels to local injury or inflammation (53-55). Cavernous malformations are associated with inflammatory cells and immune activation, although a cause-effect relationship has not been shown (56, 57). In other patients, lesions have been observed to form in brain regions following radiation injury (58). It is possible that the environmental changes induced by radiation injury are key contributors, although genetic damage is also likely to be present. In sporadic disease, prominent local venous structures have been observed that suggest an abnormal microcirculatory environment (59, 60). These observations argue for the importance of environmental "hits" in the promotion of lesion development.

The requirement for two genetic hits in each individual CCM lesion has not been shown. In familial CCM it is not uncommon for patients to have dozens or even hundreds of individual lesions. It has not been possible to test whether the burden of disease in a given patient is the consequence of greater genomic instability and more independent genetic insults, or whether local environmental cues (such as trauma, inflammation or

cytokine expression) play a critical contributing factor. One of us has been a key proponent of exploring the local influence of cytokines on modulating genetic disease (61-63). We sought to explore the interaction of genetic lesions with local environmental cues in the formation of CCM lesions in our mouse model of CCM.

Mice heterozygous for null mutations in Ccm3 will develop lesions at a frequency of 100% if given a second hit in their endothelial cells at birth (50). This model system shows widespread, early-induced somatic inactivation of Ccm3 in almost all endothelial cells of the brain, retina, and most other organs. The extent of the genetic hit exceeded that expected to occur naturally in man, yet lesions were detected in only a small minority of vessels, predominantly within the brain. The fact that one cluster of brain endothelial cells was induced to form a CCM lesion, while adjacent endothelial cells with the identical genetic lesion retained normal histology, was suggestive evidence to us that additional local environmental factors influence CCM formation.

Here we show that the induced inactivation of Ccm3 is only sufficient to induce CCM disease if delivered within a narrow susceptible window of time in early development. The induction of loss of heterozygosity within the endothelium at the time of weaning does not lead to lesion formation in either the brain or the retina. We therefore tested whether local cytokine expression could synergize with this genetic insult to induce CCM. We will show in this manuscript that delivery of vascular endothelial growth factor given along with the induced inactivation of Ccm3 in adulthood is sufficient to lead to CCM lesion formation. These data indicate that environmental factors, such as cytokines and inflammation, play an important role in the pathogenesis of this disease and suggest that targeting the brain microenvironment that facilitates CCM formation may be a

valuable strategy in ameliorating the disease.

3.4 Results and Discussion

Cerebral cavernous malformations affect two distinct populations of people. One group develops solitary lesions and lacks a family history of disease. These lesions are termed sporadic CCMs. Another group develops pathologically identical lesions in multiple, discrete locations of the central nervous system and have inheritable, familial disease. The prevailing theory to explain the basis of sporadic disease is the gradual acquisition of separate genetic insults to both copies of a CCM gene in the endothelial cells of the affected individual. This "two-hit" theory of CCM development could account for the greater likelihood of lesions in those with one inherited mutant allele and would reconcile the mechanism for lesion formation in both groups of patients into one common pathology. Support for this prevailing theory is found in both human and mouse experimentation. Surgically excised human samples from familial CCM patients have been analyzed for evidence of second genetic hits, and examples of biallelic somatic and germline mutations have been found for each of the three known CCM genes (47-49). In mice, a number of different laboratories have pursued strategies to create second genetic hits with targeted mutations of CCM genes. Using several different tamoxifen inducible Cre-recombinase systems to deliver controlled, widespread somatic endothelial "second hit" mutations at birth, our laboratory (50) and other laboratories (29) have confirmed that this mechanism is active in mice. An alternative strategy has also been pursued in which the "second hit" is the result of genomic instability in strains with high rates of spontaneous mutations (64). These naturally occurring mutations are more likely to

mimic those seen in patients. In this model the timing and nature of the second genetic hit is not controlled and is difficult to confirm, and yet the same pathology results.

Earlier work had suggested a developmental susceptibility to cavernous malformations and that the timing of the second hit might be important (29). We chose to focus our experiments on mice with mutations in Ccm3, the most severe and early onset model of CCM. The induced loss of endothelial Ccm3 at birth (P1) leads to CCM lesion formation in the brains and retinas of all mice and can be detected by MRI in the brain by 2 months of age (50). To judge the effectiveness of late induction of endothelial Ccm3 mutation, we again prepared inducible endothelial knockout mice. These mice have one germline null allele for Ccm3 with another floxed allele with exons 3 through 8 of Ccm3 flanked by loxP sites, targeted for Cre-mediated recombination. These mice were also bred to express a tamoxifen inducible Cre recombinase in endothelial cells ($Ccm3^{flox/-}$;Pdgfb-$iCreER^{T2}$) (65). Using this system, the administration of tamoxifen results in endothelial-specific loss of Ccm3. We compared mice with induction at P1 with mice induced later in development at weaning on P21. Inducible reporter gene activity demonstrated that tamoxifen treatment resulted in widespread endothelial Cre activity in the brain and retina when given at day 21 as judged by induced green fluorescence seen only in mice treated with tamoxifen (Figure 3.1A). Cavernous malformations were only seen if the genetic lesion was delivered early after birth and were not seen if induction was performed at weaning. Our previous work had shown 100% penetrance at first assessment by MRI at 2 months of age, with heavy lesion burden and some death beginning at 3 months of age (50). All mice treated at P1 were found to have CCM lesions by histology in both the brain and retina. In distinct contrast, no mice treated with

tamoxifen at P21 developed CCM lesions of either brain or retina by 7 months of age (Figure 3.1B and C), demonstrating that while loss of heterozygosity is sufficient for disease in neonatal mice, an additional lesion promoting factor or factors is necessary by P21. Delaying the second hit by a mere 3 weeks resulted in a dramatic change in the phenotype with distinctly unusual absence of lesions and mortality by 7 months in our most vulnerable genotype. Thus, the animal model data allows only a limited allowance of the two genetic hit model as the sole explanation for lesion formation, restricted to a brief, developmentally vulnerable window of time. Although the equivalent vulnerable period in humans is not clarified, it strains the imagination to think that all of the genetic hits and lesion initiation must occur early in life. Longitudinal studies in man have shown the progressive development of new lesions throughout life into adulthood (33). Our targeted genetic animal models do not provide a suitable explanation for these late-occurring lesions, which is troubling for the two genetic hit theory as the sole explanation for the gradually appearing and progressive lesions seen in familial CCM.

Clinical observations first suggested an alternative explanation to the genetic basis for new lesion development. Occasional patients have been described with an unusually rapid appearance of multiple new lesions over a short period of time. This phenomenon was observed to correlate with high serum levels of vascular endothelial growth factor (51, 52), suggesting that nongenetic, environmental triggers may act as an alternative explanation for lesion development.

To more directly test the environmental hypothesis, we designed an experiment in which the effects of both gene inactivation and angiogenesis could be assessed independently and in combination. Using viral vectors to drive expression of both Cre

recombinase and vascular endothelial growth factor (VEGF), localized central nervous system angiogenesis and/or homozygous Ccm3 mutation were induced by stereotactic injection of appropriate vectors. Four separate groups of mice were prepared (Table 1). All mice were homozygous for the floxed Ccm3 allele ($Ccm3^{flox/flox}$) and vulnerable to complete loss of Ccm3 with the expression of Cre recombinase. Each group of mice received two viral vectors, an adenovirus expressing either Cre recombinase or GFP (Adeno-Cre or Adeno-GFP), and an adeno-associated virus expressing either VEGF or beta-galactosidase (AAV-VEGF or AAV-LacZ). Thus one group received two control viruses with neither VEGF nor Cre, one group received both VEGF and Cre, and one group each received either VEGF or Cre in combination with a control virus. Injections were performed on adult mice between 6 and 8 weeks of age, and after a further 6 weeks mice were studied for vascular defects.

Using this controlled model we were able to produce CCM lesions in adult mice, but only in those receiving both the genetic insult and cytokine induction. We noticed the presence of stage 1 cavernous malformations (64) in the brains of mice treated with both Cre and VEGF (Figure 3.2A). We did not note stage 1 lesions in any other group. Neither Cre recombinase nor VEGF alone were sufficient to induce cavernous malformations. A more detailed analysis was performed by staining sections with a fluorescent endothelial specific lectin and measuring the diameter of all vessels within the microscope field (Figure 3.2B). Mice receiving both VEGF and Cre had a population of vessels greater than 80 micrometers in diameter (including both stage 1 lesions and preclinical vessel enlargement) that was not present in any other group (Figure 3.2C).

The effects of both VEGF and Cre recombinase were detected in mice that

received appropriate viral treatments. Treatment with AAV-VEGF resulted in angiogenesis and localized edema that was readily detected as a low intensity signal by MRI (Figure 3.3). There was no difference in the extent of edema whether Cre recombinase was present or not. The presence of edema obscured the ability to detect vascular lesions in mice treated with VEGF by MRI.

To confirm equal efficacy of gene inactivation, we used laser capture microdissection to remove tissue from slides focusing on the treated side of the brain. To ensure that equal regions were compared, we sampled several adjacent circular regions of brain from all sections (Figure 3.3). After purifying genomic DNA, a genomic copy number assay was performed using quantitative PCR. The region with the lowest detected copy number was assumed to include the area of peak viral expression and gene inactivation. To control for assay efficiency, we compared untreated control mice that were homozygous floxed ($Ccm3^{flox/flox}$) with mice that were heterozygous for the null allele resulting from germline Cre inactivation ($Ccm3^{flox/-}$). In the experimental samples, Cre was found to effectively reduce the Ccm3 copy number in bulk tissue obtained from the injected area. Cotreatment with VEGF did not enhance or inhibit gene inactivation, as mice receiving Cre recombinase with LacZ control vector had equal loss of Ccm3 as those receiving Cre and VEGF (Figure 3.4).

This work therefore reconciles the differing theories of CCM lesion development. We demonstrate that cytokines and genetic factors are synergistic in the development of CCM lesions. Neither a susceptible environmental insult such as localized VEGF expression, nor the induction of genetic hits in adult mice is alone sufficient to reproduce CCM pathology, but the two insults together lead to disease. Our work suggests a model

in which the genetic hits are required to give disease susceptibility, but lesion initiation occurs when the endothelium is environmentally vulnerable. In mice this vulnerability occurs naturally in early development (Figure 3.5A), and the genetic insult alone can trigger lesion development. Outside of the vulnerable developmental window the genetic lesion no longer is sufficient to induce formation of a cavernous malformation (Figure 3.5B). The late, progressive lesion development that has been seen in clinical CCM can be explained by an initial genetic predisposition with lesion initiation triggered by local environmental factors that activate the endothelium (Figure 3.5C). This model can also explain the observation that lesions in mice with widespread endothelial CCM gene inactivation at birth form in a small subset of vessels with cerebellar predominance, while the vast majority of vessels remain normal as the developmental susceptibility can be focal and brain region specific. We provide an explanation that accounts for the experimental evidence and allows the two hit theory to function at all stages of life.

These observations have important implications for the therapeutic approach to CCM disease. Currently the mainstay of therapy for CCM is surgical excision or radiological destruction of the lesion. Our previous work suggested that the genetically altered endothelium has increased activity of RhoA signaling that may be modified by therapy with the statin class of drugs (66). There are now several potential therapeutic approaches (67) suggested to modify the genetically altered endothelium of the CCM lesion, and it is hoped that a new era of medical management of CCM will prove beneficial. Here we suggest the potential of an additional therapeutic strategy to target the susceptible environment, thus protecting patients from the activation of underlying genetic susceptibilities. Antiangiogenic therapy may prove useful to prevent or delay

lesion formation or to stabilize the hemorrhage prone lesion. This strategy has already been proposed for other genetic vascular diseases, and the use of anti-VEGF therapy with bevacizumab is currently being tested in clinical trials for hereditary hemorrhagic telangiectasia (68). Additional environmental modifiers may also be found that form part of a multipronged medical approach to the treatment of CCM.

3.5 Materials and Methods

3.5.1 Mice

Mice with a conditional (floxed) allele for Ccm3 and a germline deleted Ccm3 allele were generated previously. The endothelial inducible Cre recombinase used in this model (Pdgfb-iCreERT2) were used previously (50) and were originally obtained via Holger Gerhart (London Research Institute – Cancer Research UK, London, United Kingdom) from Marcus Fruttiger (University College London Institute of Ophthalmology, London, United Kingdon). Reporter mice expressing baseline red fluorescence with a Cre-inducible green fluorescence (Tomato-GFP mice) were obtained from Jackson Laboratories (Bar Harbor, ME).

3.5.2 Reporter Gene Expression

Brain and intact eyes were prepared for cross-sectional analysis by embedding into OCT for frozen sections at 10 μm thickness. Sections were counterstained with DAPI and mounted with Dako Faramount Aqueous mounting media. Intrinsic fluorescence from tomato-red and GFP expression or from DAPI counterstain was detected using the Nikon AR1 confocal microscope using a 60X objective (with oil)

using NIS Elements software.

3.5.3 Mouse MRI Studies

Both live and postmortem mouse brain MRI studies were performed as described previously (50). All MRI experiments were conducted on a 7T Bruker Biospec 70/30 USR scanner (Bruker Biosin MRI Inc.) equipped with a BGA12S gradients set. A combination of volume-transmit-only radio frequency coil (internal diameter 72 mm) and a quad-surface-receive-only coil (internal diameter 1.5 cm) were used. For live scans, mice were anesthetized with 2.5% isoflurane and then placed into the scanner on top of a circulating heated water. During the scans, mice were monitored for temperature and respiration, with isoflurane concentration and water bath temperature adjusted to maintain a body temperature between 35.8 and 37.6 °C and respiration between 75 and 100 breaths/minute. A gradient recalled echo sequence was used to acquire coronal slices spanning the whole brain. Sequence parameters were as follows: repetition time, 328 ms; echo time, 5.4 ms; flip-angle, 40°; 12 averages, in-plane-resolution 125 μm x 125 μm; and slice thickness 0.5 mm. For postmortem specimens, mouse skulls were fixed in 4% formaldehyde for at least 3 days before the brain was imaged with the skull intact. High resolution 3D gradient echo was acquired using the same scanner configuration described above, with isotopic voxel size of 78 μm x 78 μm x 78 μm over 9 hours. Other sequence parameters were as follows: repetition time, 250 ms; echo time, 7.5 ms; flip angle, 30°; and 2 averages. Two independent reviewers blinded to treatment group reviewed the MRI studies.

3.5.4 Retinal Processing

Eyes were enucleated and fixed overnight in 4% paraformaldehyde at 4 °C. Retinas were then dissected and stained with Alexa Fluor Isolectin GS-IB4 (Invitrogen). After staining, retinas were placed into PBS, cut four times to section the cup into leaflets, and then flat-mounted onto slides using Dako Faramount Aqueous mounting media. Images were acquired on a Nikon AR1 confocal microscope with a 10X objective and stitched into a 3x3 montage using the NIS Elements software.

3.5.5 Viral Vectors Preparation and Transduction in the Mouse Brain

Adenoviral vectors with a CMV promoter driving Cre recombinase (Adeno-Cre) and control adenovector expressing green fluorescent protein (Adeno-GFP) were purchased from Vector Biolabs (Philadelphia, PA). Adeno-associated viral vectors containing vascular endothelial growth factor (AAV-VEGF) and ß-galactosidase (AAV-LacZ) were prepared (69) by using a three plasmid cotransfection system. Briefly, recombinant pAAV plasmids were cotransfected with two helper plasmids to 293 cells using the calcium phosphate precipitate method. Two helper plasmids, one with adenoviral VA, E2A, and E4 regions and the other with the AAV rep and AAV serotype one cap genes (provided by Xiao Xiao, University of North Carolina), were cotransfected with AAV plasmids into HEK 293 cells to package the AAV vector. Cell lysate was produced using three freeze-and-thaw cycles 3 days after the transfection. AAV vector was purified by CsCl2 centrifugation. Viral titers were determined by dot blot analysis of the DNA content.

Stereotactic injections of combination adenoviral and adeno-associated viral

vectors were performed as described previously (70). Following induction of anesthesia with isoflurane, the mice were placed in a stereotactic frame with a holder (David Kopf Instruments, Tujunga, CA), and a burr hole was drilled in the pericranium 2 mm lateral to the sagittal suture and 1 mm posterior to the coronal suture. A 3 µl viral suspension containing 2 x 10^7 plaque forming unit (PFU) adenoviral vectors and 2 x 10^9 genome copies (gcs) of AAV viral vectors were stereotactically injected into the right basal ganglia at a rate of 0.2 µl per minute using a Hamilton syringe. The needle was withdrawn after 10 minutes and the wound closed with a suture.

3.5.6 Histologic and Fluorescent Stains

Following postmortem MRI, mouse brains were prepared and stained for H&E as described previously (50). Sections of brain were prepared at 5µm thickness, and H&E staining was performed according to classical protocols. Photomicrographs were obtained using a Zeiss Axiophot 2 microscope with 10x objective with an Axiocam HRc camera and Axiovision software. Sections were also stained for fluorescein-lycopersicin esculentum lectin (Vector Laboratories, Burlingame, CA). Two sections per mouse brain, 1mm rostral and 1mm caudal of the injection site, were chosen. The angiogenic regions were imaged using a Lieca microscope with 10x objective and SPOT Camera and Software. Vessel diameters were analyzed using NIH Image 1.63 software by observers blinded to treatment group.

3.5.7 Genomic DNA Quantitative PCR for Copy Number

Paraffin sections of mouse brain were analyzed for Ccm3 gene copy number. Serial slides were analyzed for evidence of injection. Histologic stains were used on every fifth slide to define evidence of gliosis, or minimal injection injury. Bulk samples of brain tissue from the intervening sections were taken from the injected region for genomic DNA extraction using an Arcturus Veritas laser capture dissecting microscope to cut a standard pattern of five precise circular fields that were later scraped off of the slide with a scalpel into sample buffer. Images of the sections following tissue removal were obtained using the same system with a 2X objective. DNA was extracted using a Qiaquick PCR DNA extraction kit from Qiagen (Germantown, MD). A Ccm3 copy number assay sensitive to the known mutation induced by Cre recombinase was obtained from Applied Biosystems (Life Technologies, Grand Island, NY) and used for analysis of recombination efficacy. The assay was validated by comparison of DNA from control mice without viral vectors ($Ccm3^{flox/flox}$ compared to $Ccm3^{Flox/-}$).

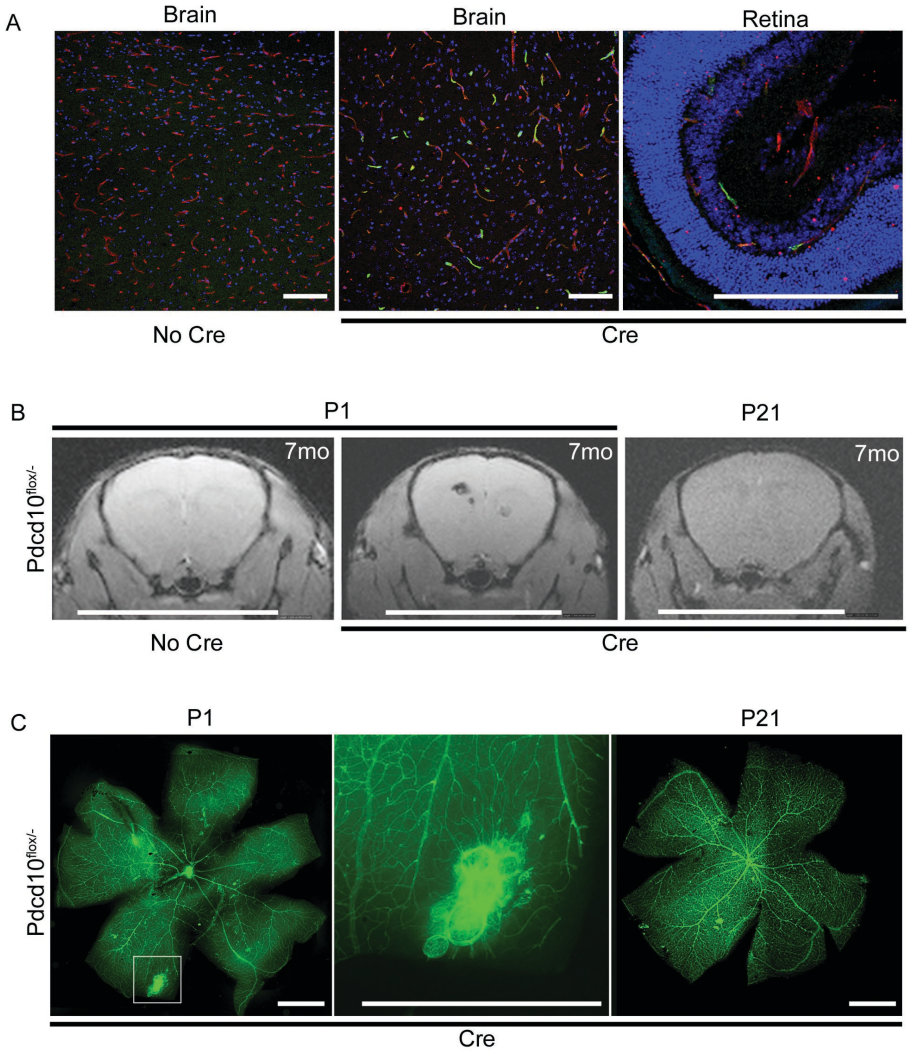

Figure 3.1. Late induction of gene deletion is insufficient for cavernous malformations. A. Tamoxifen treatment of Tomato-GFP;Pdgfb-iCreER^{T2} mice at weaning results in endothelial Cre activity within the brain and retina. Cavernous malformations form in the brains (B) and retina (C) of Ccm3$^{flox/-}$;Pdgfb-iCreER^{T2} mice treated with tamoxifen at birth (P1) but not at weaning (P21). Scale bars = 100 μm in A, 1 mm in B and C.

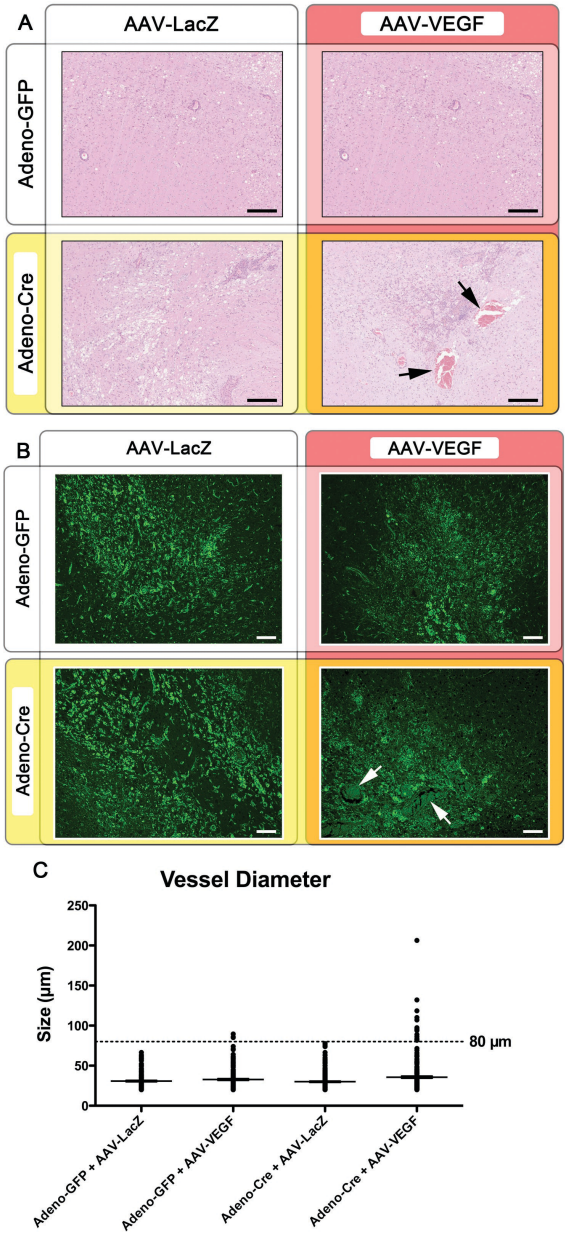

Figure 3.2. VEGF potentiates cavernous malformation development following the loss of Ccm3. A. H&E staining of mouse brain. Type 1 CCM lesions are apparent only from the brains of mice receiving both Cre recombinase and VEGF viral vectors. B. Lectin staining also identifies the lesions and allows quantification of vessel diameter. C. The combination of VEGF and Cre recombinase (group D) results in a population of enlarging vessels including cavernous malformations. Scale bars = 200 µm in A, 100 µm in B.

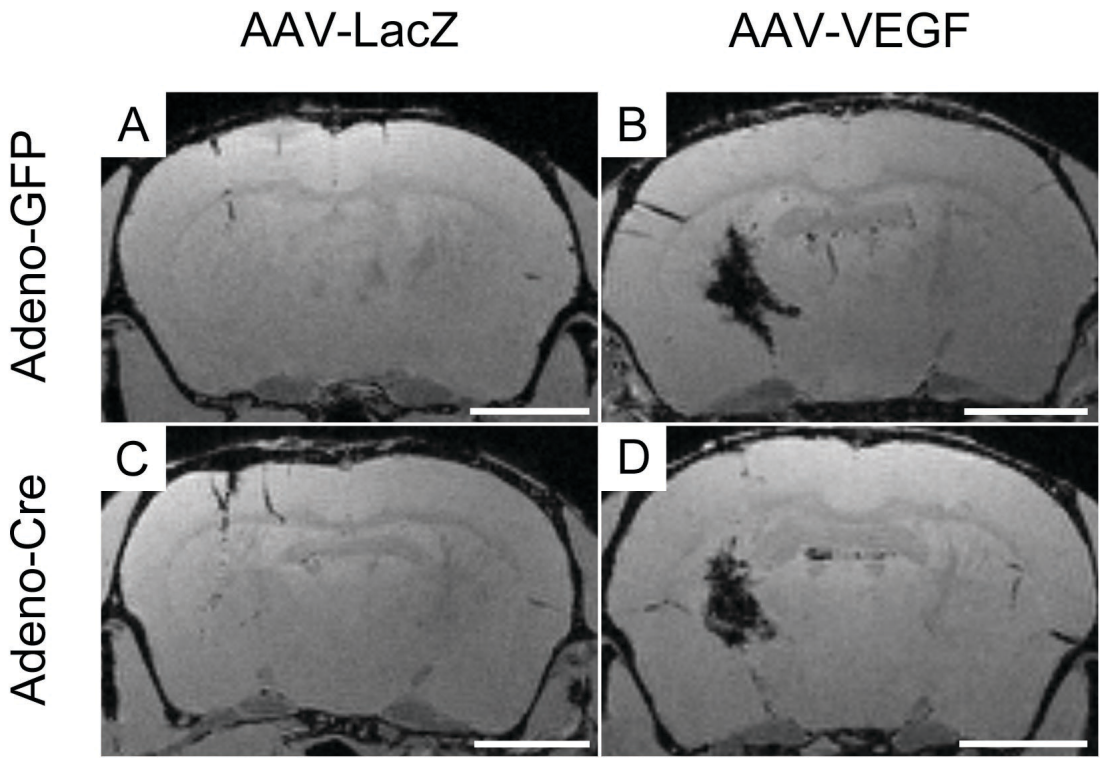

Figure 3.3. Viral vector driven expression of VEGF results in gliosis and edema independent of Cre expression. Mice given adeno-associated viral driven VEGF have localized edema and gliosis at the injection site, obscuring the MRI appearance of cavernous malformations.

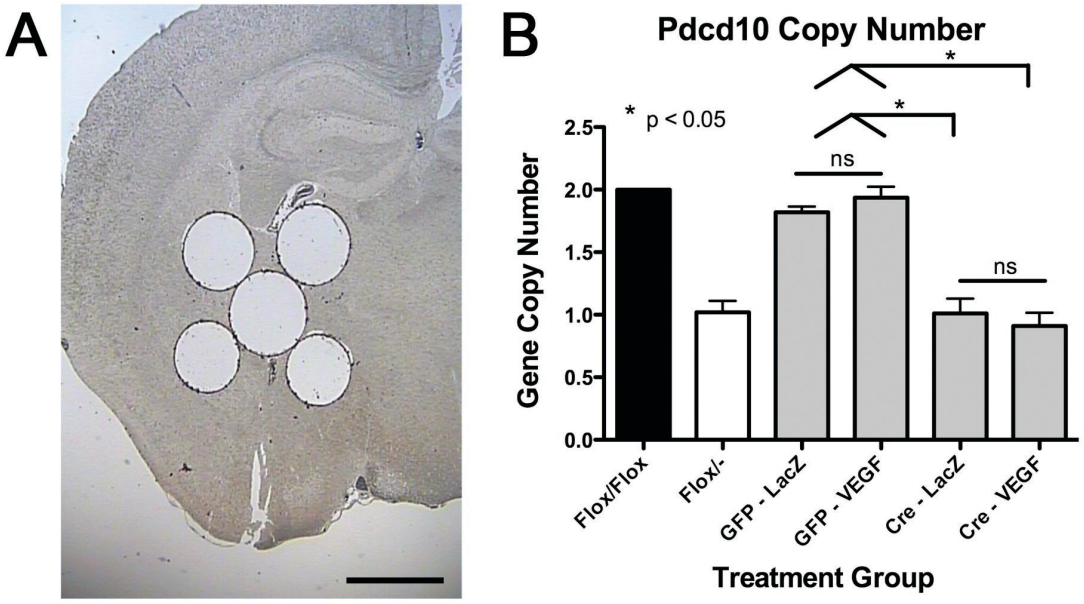

Figure 3.4. Viral vector driven expression of Cre recombinase results in equivalent gene deletion independent of VEGF expression. A. DNA was purified from a standard pattern of samples from the injected brain region. B. A Ccm3 gene copy number assay correctly identifies the copy number of control ($Ccm3^{flox/flox}$ and $Ccm3^{flox/-}$) mice. Copy number is decreased only in mice receiving Adeno-Cre. Scale bar = 200 μm.

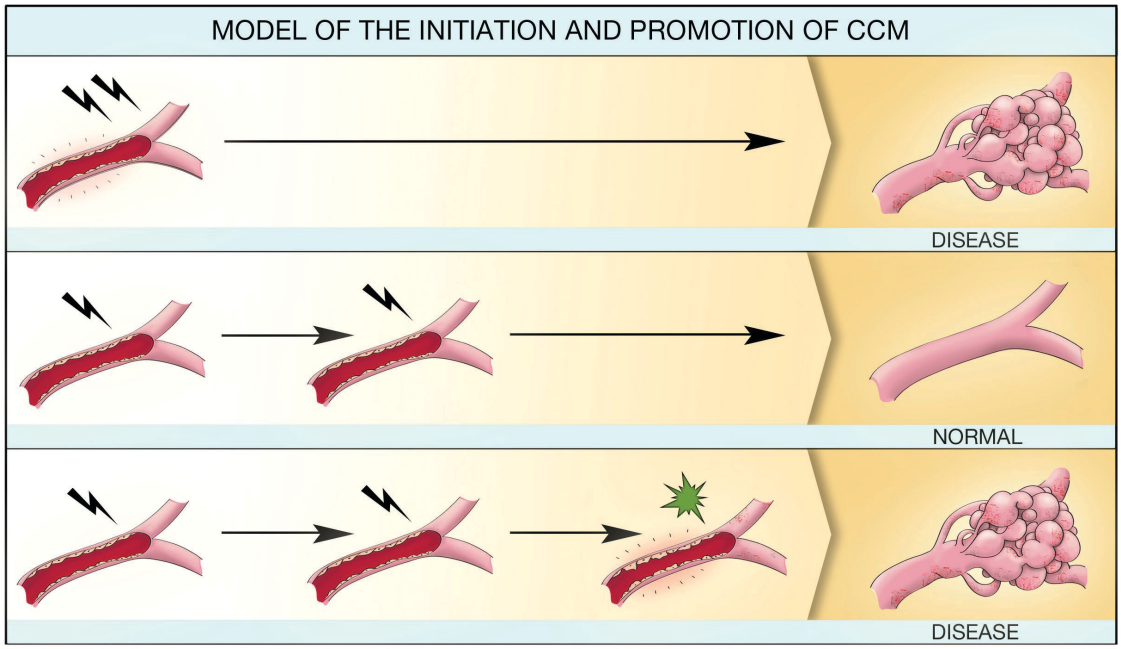

Figure 3.5. Environmental and genetic synergy in CCM lesion formation. A. Two genetic hits at a developmentally vulnerable period is sufficient to induce CCM lesion formation. B. A second genetic hit that occurs later in life, outside of the developmentally vulnerable time window does not result in disease unless a subsequent environmental insult activates the process of lesion formation in the genetically susceptible vessel.

3.6 References

1 Labauge, P., Brunereau, L., Levy, C., Laberge, S. and Houtteville, J.P. (2000) The natural history of familial cerebral cavernomas: a retrospective MRI study of 40 patients. *Neuroradiology*, **42**, 327-332.

2 Kupersmith, M.J., Kalish, H., Epstein, F., Yu, G., Berenstein, A., Woo, H., Jafar, J., Mandel, G. and De Lara, F. (2001) Natural history of brainstem cavernous malformations. *Neurosurgery*, **48**, 47-53; discussion 53-44.

3 Vernooij, M.W., Ikram, M.A., Tanghe, H.L., Vincent, A.J., Hofman, A., Krestin, G.P., Niessen, W.J., Breteler, M.M. and van der Lugt, A. (2007) Incidental findings on brain MRI in the general population. *N. Engl. J. Med.*, **357**, 1821-1828.

4 Porter, P.J., Willinsky, R.A., Harper, W. and Wallace, M.C. (1997) Cerebral cavernous malformations: natural history and prognosis after clinical deterioration with or without hemorrhage. *J. Neurosurg.*, **87**, 190-197.

5 Otten, P., Pizzolato, G.P., Rilliet, B. and Berney, J. (1989) A propos de 131 cas d'angiomes caverneux (cavernomes) du S.N.C. repérés par l'analyse rétrospective de 24 535 autopsies. *Neurochirurgie*, **35**, 82-83, 128-131.

6 Laberge-le Couteulx, S., Jung, H.H., Labauge, P., Houtteville, J.P., Lescoat, C., Cecillon, M., Marechal, E., Joutel, A., Bach, J.F. and Tournier-Lasserve, E. (1999) Truncating mutations in CCM1, encoding KRIT1, cause hereditary cavernous angiomas. *Nat. Genet.*, **23**, 189-193.

7 Sahoo, T., Johnson, E.W., Thomas, J.W., Kuehl, P.M., Jones, T.L., Dokken, C.G., Touchman, J.W., Gallione, C.J., Lee-Lin, S.Q., Kosofsky, B. *et al.* (1999) Mutations in the gene encoding KRIT1, a Krev-1/rap1a binding protein, cause cerebral cavernous malformations (CCM1). *Hum. Mol. Genet.*, **8**, 2325-2333.

8 Serebriiskii, I., Estojak, J., Sonoda, G., Testa, J.R. and Golemis, E.A. (1997) Association of Krev-1/rap1a with Krit1, a novel ankyrin repeat-containing protein encoded by a gene mapping to 7q21-22. *Oncogene*, **15**, 1043-1049.

9 Liquori, C.L., Berg, M.J., Siegel, A.M., Huang, E., Zawistowski, J.S., Stoffer, T., Verlaan, D., Balogun, F., Hughes, L., Leedom, T.P. *et al.* (2003) Mutations in a gene encoding a novel protein containing a phosphotyrosine-binding domain cause type 2 cerebral cavernous malformations. *Am. J. Hum. Genet.*, **73**, 1459-1464.

10 Denier, C., Goutagny, S., Labauge, P., Krivosic, V., Arnoult, M., Cousin, A., Benabid, A.L., Comoy, J., Frerebeau, P., Gilbert, B. *et al.* (2004) Mutations within the MGC4607 gene cause cerebral cavernous malformations. *Am. J. Hum. Genet.*, **74**, 326-337.

11 Uhlik, M.T., Abell, A.N., Johnson, N.L., Sun, W., Cuevas, B.D., Lobel-Rice, K.E., Horne, E.A., Dell'Acqua, M.L. and Johnson, G.L. (2003) Rac-MEKK3-MKK3 scaffolding for p38 MAPK activation during hyperosmotic shock. *Nat. Cell Biol.*, **5**, 1104-1110.

12 Bergametti, F., Denier, C., Labauge, P., Arnoult, M., Boetto, S., Clanet, M., Coubes, P., Echenne, B., Ibrahim, R., Irthum, B. *et al.* (2005) Mutations within the programmed cell death 10 gene cause cerebral cavernous malformations. *Am. J. Hum. Genet.*, **76**, 42-51.

13 Knudson, A.G., Jr. (1971) Mutation and cancer: statistical study of retinoblastoma. *Proc. Natl. Acad. Sci. U S A*, **68**, 820-823.

14 Kehrer-Sawatzki, H., Wilda, M., Braun, V.M., Richter, H.P. and Hameister, H. (2002) Mutation and expression analysis of the KRIT1 gene associated with cerebral cavernous malformations (CCM1). *Acta. Neuropathol. (Berl)*, **104**, 231-240.

15 Gault, J., Shenkar, R., Recksiek, P. and Awad, I.A. (2005) Biallelic somatic and germ line CCM1 truncating mutations in a cerebral cavernous malformation lesion. *Stroke*, **36**, 872-874.

16 Akers, A.L., Johnson, E., Steinberg, G.K., Zabramski, J.M. and Marchuk, D.A. (2009) Biallelic somatic and germline mutations in cerebral cavernous malformations (CCMs): evidence for a two-hit mechanism of CCM pathogenesis. *Hum. Mol. Genet.*, **18**, 919-930.

17 Gault, J., Awad, I.A., Recksiek, P., Shenkar, R., Breeze, R., Handler, M. and Kleinschmidt-DeMasters, B.K. (2009) Cerebral cavernous malformations: somatic mutations in vascular endothelial cells. *Neurosurgery*, **65**, 138-144; discussion 144-135.

18 Chan, A.C., Drakos, S.G., Ruiz, O.E., Smith, A.C., Gibson, C.C., Ling, J., Passi, S.F., Stratman, A.N., Sacharidou, A., Revelo, M.P. *et al.* (2011) Mutations in 2 distinct genetic pathways result in cerebral cavernous malformations in mice. *J. Clin. Invest.*, **121**, 1871-1881.

19 Boulday, G., Rudini, N., Maddaluno, L., Blecon, A., Arnould, M., Gaudric, A., Chapon, F., Adams, R.H., Dejana, E. and Tournier-Lasserve, E. (2011) Developmental timing of CCM2 loss influences cerebral cavernous malformations in mice. *J. Exp. Med.*, **208**, 1835-1847.

20 Abe, T., Morishige, M., Ooba, H., Kamida, T., Fujiki, M., Kobayashi, H., Sakoda, T. and Kimba, Y. (2009) The association between high VEGF levels and multiple probable punctuate cavernous malformations. *Acta. Neurochirurgica*, **151**, 855-859.

21 Jung, K.H., Chu, K., Jeong, S.W., Park, H.K., Bae, H.J. and Yoon, B.W. (2003)

Cerebral cavernous malformations with dynamic and progressive course: correlation study with vascular endothelial growth factor. *Arch. Nerol.*, **60**, 1613-1618.

22 Cobbs, C.S., Chen, J., Greenberg, D.A. and Graham, S.H. (1998) Vascular endothelial growth factor expression in transient focal cerebral ischemia in the rat. *Neurosci. Lett.*, **249**, 79-82.

23 Lennmyr, F., Ata, K.A., Funa, K., Olsson, Y. and Terent, A. (1998) Expression of vascular endothelial growth factor (VEGF) and its receptors (Flt-1 and Flk-1) following permanent and transient occlusion of the middle cerebral artery in the rat. *J. Neuropath. Exp. Neur.*, **57**, 874-882.

24 Argaw, A.T., Asp, L., Zhang, J., Navrazhina, K., Pham, T., Mariani, J.N., Mahase, S., Dutta, D.J., Seto, J., Kramer, E.G. *et al.* (2012) Astrocyte-derived VEGF-A drives blood-brain barrier disruption in CNS inflammatory disease. *J. Clin. Invest.*, **122**, 2454-2468.

25 Shenkar, R., Shi, C., Check, I.J., Lipton, H.L. and Awad, I.A. (2007) Concepts and hypotheses: inflammatory hypothesis in the pathogenesis of cerebral cavernous malformations. *J. Neurosurg.*, **61**, 693-702; discussion 702-693.

26 Shi, C., Shenkar, R., Batjer, H.H., Check, I.J. and Awad, I.A. (2007) Oligoclonal immune response in cerebral cavernous malformations. Laboratory investigation. *J. Neurosurgery.*, **107**, 1023-1026.

27 Larson, J.J., Ball, W.S., Bove, K.E., Crone, K.R. and Tew, J.M., Jr. (1998) Formation of intracerebral cavernous malformations after radiation treatment for central nervous system neoplasia in children. *J. Neurosurg.*, **88**, 51-56.

28 Clatterbuck, R.E., Elmaci, I. and Rigamonti, D. (2001) The juxtaposition of a capillary telangiectasia, cavernous malformation, and developmental venous anomaly in the brainstem of a single patient: case report. *J. Neurosurg.*, **49**, 1246-1250.

29 Petersen, T.A., Morrison, L.A., Schrader, R.M. and Hart, B.L. (2010) Familial versus sporadic cavernous malformations: differences in developmental venous anomaly association and lesion phenotype. *Am. J. Neuroradiol.*, **31**, 377-382.

30 Xu, B., Wu, Y.Q., Huey, M., Arthur, H.M., Marchuk, D.A., Hashimoto, T., Young, W.L. and Yang, G.Y. (2004) Vascular endothelial growth factor induces abnormal microvasculature in the endoglin heterozygous mouse brain. *J. Cereb. Flow Metab.*, **24**, 237-244.

31 Hao, Q., Zhu, Y., Su, H., Shen, F., Yang, G.Y., Kim, H. and Young, W.L. (2010) VEGF induces more severe cerebrovascular dysplasia in endoglin than in Alk1 mice. *Transl. Stroke Res.*, **1**, 197-201.

32 Choi, E.J., Walker, E.J., Shen, F., Oh, S.P., Arthur, H.M., Young, W.L. and Su, H. (2012) Minimal homozygous endothelial deletion of Eng with VEGF stimulation is sufficient to cause cerebrovascular dysplasia in the adult mouse. *Cerebrovasc. Dis.*, **33**, 540-547.

33 McDonald, D.A., Shenkar, R., Shi, C., Stockton, R.A., Akers, A.L., Kucherlapati, M.H., Kucherlapati, R., Brainer, J., Ginsberg, M.H., Awad, I.A. *et al.* (2010) A novel mouse model of cerebral cavernous malformations based on the two-hit mutation hypothesis recapitulates the human disease. *Hum. Mol. Genet.*, **20**, 211-222.

34 Claxton, S., Kostourou, V., Jadeja, S., Chambon, P., Hodivala-Dilke, K. and Fruttiger, M. (2008) Efficient, inducible Cre-recombinase activation in vascular endothelium. *Genesis*, **46**, 74-80.

35 Whitehead, K.J., Chan, A.C., Navankasattusas, S., Koh, W., London, N.R., Ling, J., Mayo, A.H., Drakos, S.G., Marchuk, D.A., Davis, G.E. *et al.* (2009) The cerebral cavernous malformation signaling pathway promotes vascular integrity via Rho GTPases. *Nat. Med.*, **15**, 177-184.

36 McDonald, D.A., Shi, C., Shenkar, R., Stockton, R.A., Liu, F., Ginsberg, M.H., Marchuk, D.A. and Awad, I.A. (2012) Fasudil decreases lesion burden in a murine model of cerebral cavernous malformation disease. *Stroke*, **43**, 571-574.

37 Dupuis-Girod, S., Ginon, I., Saurin, J.C., Marion, D., Guillot, E., Decullier, E., Roux, A., Carette, M.F., Gilbert-Dussardier, B., Hatron, P.Y. *et al.* (2012) Bevacizumab in patients with hereditary hemorrhagic telangiectasia and severe hepatic vascular malformations and high cardiac output. *JAMA*, **307**, 948-955.

38 Shen, F., Walker, E.J., Jiang, L., Degos, V., Li, J., Sun, B., Heriyanto, F., Young, W.L. and Su, H. (2011) Coexpression of angiopoietin-1 with VEGF increases the structural integrity of the blood-brain barrier and reduces atrophy volume. *J. Cereb. Flow Metab.*, **31**, 2343-2351.

39 Walker, E.J., Su, H., Shen, F., Choi, E.J., Oh, S.P., Chen, G., Lawton, M.T., Kim, H., Chen, Y., Chen, W. *et al.* (2011) Arteriovenous malformation in the adult mouse brain resembling the human disease. *Ann. Neurol.*, **69**, 954-962.

CHAPTER 4

ENDOTHELIA EXTRUDE DYING CELLS TO MAINTAIN A CONSTANT BARRIER

In addition to myself the other authors on this paper include Michael Redd, Aubrey C Chan, Yapeng Gu, Dean Y Li, and Jody Rosenblatt. I participated in experimental design, cell culture experiments, zebrafish experiments, data analysis and manuscript preparation.

4.1 Authors

Title: Endothelia extrude dying cells to maintain a constant barrier

Authors: Tara M. Mleynek[1,3], Michael Redd[2], Aubrey C Chan[1,3], Yapeng Gu, Dean Y. Li[1,2,4,5], Jody Rosenblatt[3]

[1]Department of Molecular Medicine, University of Utah, Salt Lake City 84112, USA
[2]Flourescence Imaging Core, University of Utah, Salt Lake City 84112, USA
[3]Department of Oncological Sciences, University of Utah, Salt Lake City 84112, USA
[4]Division of Cardiovascular Medicine, Salt Lake City 84132, USA
[5]The Key Laboratory for Human Disease Gene Study of Sichuan Province, Institute of Laboratory Medicine, Sichuan Academy of Medical Sciences & Sichuan Provincial People's Hospital, Chengdu, Sichuan 610072, China

4.2 Abstract

Endothelial cells are a critical component of the vascular system. These cells act in a monolayer and are responsible for regulation of transport and provide a barrier function. It is therefore critical to maintain the integrity of this monolayer during apoptotic challenge. We sought to address the question of how endothelial cells manage apoptosis in order to protect the barrier. We demonstrate that endothelial cells use the process of cellular extrusion to remove an apoptotic cell from the monolayer without barrier disruption. We go on to show that this signaling mechanism used is based on an S1P-Rho axis, conserved across both the epithelium and the endothelium. Thus, our findings provide a mechanism for barrier preservation and open up potential avenues for therapeutics in diseases of vascular leak.

4.3 Introduction

The vasculature is an essential system that delivers blood and nutrients throughout the body while also acting as a barrier between blood and the surrounding tissues. This barrier is both physical, separating a fluid environment from a solid environment, as well as chemical, maintaining osmotic and nutrient balance in both areas (1). Lining the vessels in a tight monolayer are endothelial cells, the key players in the regulation of vascular barrier function. When barrier function is disrupted, fluid can leak into the surrounding tissues causing edema, inflammation, and tissue damage (2). Several diseases are known to have a defective endothelial barrier. One example is rheumatoid arthritis, where defects in cellular signaling and endothelial junctions leads to fluid leak into the synovial joints, where it causes swelling and inflammation (3). Another example can be found in cancer where tumors promote the growth of leaky vessels and allow for a greater rate of metastasis (4). Part of the problem presented in these situations comes from a direct threat on the endothelium. Several insults, such as inflammatory cytokines or reactive oxygen species, bombard the endothelium and can induce apoptosis (5). An apoptotic event can result in a compromised barrier as the cell surrenders its role in the monolayer and loses structural integrity. Therefore, being able to strike a balance between managing barrier function and managing apoptosis is key in maintaining endothelial function.

Endothelial cells are not the only cells responsible for barrier function within the body. Epithelial cells also exact a similar role and work to form a barrier for the internal organs as well as the outside of the body. We previously found that epithelia maintain a constant barrier even when up to 40% of the cells comprising them die by a process

termed “cell extrusion” (6). To extrude a cell that is fated to die emits a lipid Sphingosine 1-Phosphate (S1P), which binds the S1P receptor 2 (S1P2) in the neighboring cells, which trigger an actin and myosin II ring to form and contract around the cell, squeezing it out and simultaneously preventing any gaps that might have formed from the dying cell. Typically, epithelial cells die by first extruding alive and later dying due to loss of survival signaling from losing contact with the surrounding cells and matrix (7). However, apoptotic stimuli also triggers cells undergoing apoptosis to extrude early in the pathway before they lose membrane integrity (6, 8). Thus, epithelial extrusion successfully removes an apoptotic cell before it compromises the monolayer, preserving the barrier function. Consequently, we wondered if endothelia use a similar strategy that epithelia use to cope with cells dying within their ranks.

Here we demonstrate that apoptotic extrusion does occur in the endothelia. We found that endothelial cells in culture and in zebrafish embryos extrude cells targeted to die. Furthering our study, we show that endothelial cells use an S1P-S1PR2-RhoA pathway to activate extrusion, indicating a conserved mechanism between epithelial and endothelia. Together this suggests the process of extrusion enables endothelia to keep a protective barrier as cells die and opens up a new avenue in studying vascular leak in the context of disease.

4.4 Results

4.4.1 Endothelia Extrude Apoptotic Cells

To investigate if extrusion occurs in the endothelium because the intrinsic rates of endothelial cell turnover is low, we investigated whether apoptotic stimuli cause

endothelial cells to extrude. We induced apoptosis in an endothelial monolayer by exposure to UV light. Human Umbilical Vein Endothelial Cells (HUVECs) grown on glass coverslips to confluence were exposed to UV-C to activate the intrinsic apoptotic pathway and culture for 2 hours. Immunofluorescence shows that HUVEC monolayers extruded active caspase-3-positive apoptotic cells, as an actin ring forms around and below them without any obvious gaps in the monolayer. While both untreated endothelial cells extruded cells, the number of extrusions greatly increased with UV-C treatment suggesting that, similar to epithelia, endothelia extrude cells during normal homeostatic turnover and in response to apoptotic stimuli (Figure 4.1A-D). To confirm that the actin ring was actually contracting and that no gaps were produced as cells were extruded, we filmed HUVECs cells expressing LifeAct, a protein that labels filamentous actin. Our movies indicate that as cells begin to die and contract, an actin ring forms in adjacent cells, which contracts around the dying cell to push it out of the monolayer (Supplemental Movie 1, Figure 4.1E). Further, no gaps appear throughout this process, even when five cells have been extruded. Thus, endothelia extrude apoptotic cells by the same actin ring closure described in the epithelium.

4.4.2 Barrier Function is Preserved After Induction of Apoptosis

While no gaps are apparent during the extrusion process in our films, to functionally test whether the barrier was preserved as cells die, we directly measured barrier function by electrical resistance. Even when 13% of the cells were measured to die by immunfluorescence (Figure 4.2A-F), the barrier function was maintained, as indicated by the high electrical resistance measured by Electric Cell-substrate Impedance

Sensing (ECIS). This technique allows for sensitive detection of any disruption to monolayer integrity, as when cell junctions were disrupted by either EGTA or by an adherens junction antibody, this resistance was lost (Figure 4.2G). By contrast, both untreated cells and UV-C-exposed cells maintained their resistance up to 6 hours. Similarly, extruding epithelial monolayers treated with UV-C maintained high electrical impedence over a 6-hour period (Figure 4.2H).

4.4.3 Endothelial Extrusion Requires S1P Signaling

Given that endothelia extrude dying cells, we next wondered if they use the same S1P-S1P2-Rho-dependent pathway identified for controlling epithelial cell extrusion. For an epithelial cell to extrude, it produces and emits S1P, which binds to S1P2, triggering the localized activation of Rho via the p115RhoGEF pathway (8, 9). Blocking any step in this pathway leads to dying cells stuck within the monolayer and, eventually, the formation of epithelial gaps (6, 9)

In order to test if the endothelium uses the S1P-S1P2R-Rho pathway during extrusion, we treated endothelial monolayers with inhibitors at each step. Inhibition of Rho with the downstream ROCK inhibitor Y27632 treatment causes up to a 90% reduction in successful extrusion in both nontreated and UV-C-treated HUVEC monolayers (Figure 4.3A). Additionally, preventing the synthesis of S1P with a sphingosine-1-kinase inhibitor or preventing the interaction of S1P with S1P2 by using the S1PR2 specific agonist JTE-013 lead to a 60% decrease in successful extrusions (Figure 4.3C). Defective extrusion is indicated by sample images showing an uncontracted actin ring around a caspase-3-positive cell, where the DNA of the dying cell

lies in the same plane as the surrounding endothelial cell neighbors (Figure 4.3B,D). These data demonstrate that endothelial extrusion uses the same S1P-S1P2-RhoA pathway to trigger ring formation and closure as identified for epithelia.

4.4.4 Extrusions Occur in Vivo

While we have observed endothelial cell extrusion in cultured endothelial monolayers, to be convinced of its physiological relevance, we needed to determine if endothelial cell extrusion occurs *in vivo*. To investigate if endothelia extrude *in vivo*, we turned to zebrafish embryos, which are translucent so that we can image cell movements live. Other model organisms lack developed vasculature or the ability to readily access cells for filming. Further, we have previously used zebrafish embryonic epidermis to follow epithelial cell extrusion live (8) due to how easy they are to visualize. We chose to film the zebrafish common cardinal veins (CCVs), which develop in large flat endothelial sheets so that individual cells are easy to film and used the kdrl:GFP zebrafish line, which primarily labels the endothelium. We targeted individual cells to die with an infrared laser and then followed their fate by imaging for the course of 8 hours. Similar to videos of endothelial cell extrusion in culture, CCV endothelial cells targeted to die also extruded by cell contraction (Figure 4.4). Therefore, endothelia extrude cells targeted to die using the same signaling and mechanism described for epithelial cell extrusion.

4.5 Discussion

Understanding how the endothelium can maintain a barrier function despite a continuous barrage of apoptotic stimuli is critical to understanding how diseases of

vascular leak can arise. Our work demonstrates that the endothelium can respond to apoptotic stress via a mechanism of cellular extrusion. Furthermore, we indicate a mechanistic overlap in extrusion signaling between endothelia and epithelia. The occurrence of this phenomenon suggests that extrusion, or the disruption of extrusion, may be a critical component to vascular disease and provides insight into S1P and Rho signaling.

S1P is known to regulate vascular development. A knockout mouse model for S1PR2 shows vascular remodeling defects in the inner ear as well as neovascularization after hyperoxia (9, 10). RhoA also plays a critical role in the preservation of endothelial function and vascular development. For example, the disease Cerebral Cavernous Malformation (CCM), can present with a hyperactivation of RhoA and resulting vascular leak within the brain (11). It is therefore possible that disruption of these signaling pathways can also disrupt endothelial extrusion, contributing to or giving rise to these disease states.

In addition, our work may inform the process of heamatopeosis. Previous work by Philipe Herbomels has described a similar phenomenon known as endothelial heamotpoetic transition. This is a process where endothelial cells bend and bud off from the aortic wall into the subaortic space, located on the basal side of endothelial cells (12). Directionality of extrusion has been described in the epithelia, with cells extruding either apically or basally. We have so far observed either apical or basal extrusion occurring singularly depending on the system. In cell culture this may be due to endothelial layers being far thinner than epithelial layers, biasing the cells to extrude apically. While our observations in vivo are limited to basal extrusion, this is potentially influenced by the

curvature of the CCV. The inherent, flat architecture of endothelial cells may also contribute. Microtubules within the epithelial cells dictate extrusion direction by either contracting at the apical surface of the cell (basal extrusion) or by diving down to contract at the basal surface of the cell (apical extrusion) (8). It is therefore possible that endothelial cells are too planar for microtubule relocation.

Taken together, our results combined with the vast field of vascular leak suggest that endothelial extrusion may open up a new field of endothelial biology, and further study is required to examine how pervasive a role this concept has.

4.6 Materials and Methods

4.6.1 Zebrafish

Housing and experiments were conducted according to IACUC protocol. The zebrafish line kdrl:GFP was a gift from Brent Bisgrove. Embryos were filmed starting between 20 and 22hpf for 8 hours while anesthetized with tricane. Fish were mounted in 1% low-melt agarose with phenylthriourea.

4.6.2 Cell Culture

Human Microvascular Endothelial Cells (HMVEC-d, Lonza CC-2543) and Human Umbilical Vein Cells (HUVEC, Lonza C2519A) were cultured according to manufacturer's instructions. Madin Darby Canine Kidney Cells (MDCK II) and HEK293T cells were cultured in DMEM high glucose with 5% FBS and 100μg/mL penicillin/streptomycin (all from Invitrogen) according to manufacturer's instructions.

4.6.3 Immunofluorescence

Cells were grown to confluency on fibronectin-coated glass cover slips and fixed using 4% PFA at 37°C for 20 minutes. Cells were then stained as previously described (Rosenblatt 2009) using Alexa Fluor 568 Phalloidin (Life Technologies A12380) at a 1:100 dilution and Rabbit Anti-Active Caspase-3 (BD Pharmingen 559565) at a 1:1000 dilution followed by Alexa Fluor 488 Anti-Rabbit (Life Technologies A11034) at a 1:100 dilution. Cover slips were mounted using Prolong Gold Antifade Mountant with DAPI (Life Technologies P36930).

4.6.4 Imaging

Fluorescent micrographs were taken using the Nikon AR1 microscope. Visual quantification of cells was done using the Leica TCS SP5 microscope. Live cell time-lapse imaging was done using the Olympus IX81 automated microscope. Live imaging and IR ablations in zebrafish were done using the Prairie two-photon microscope.

4.6.5 Barrier Function Assay

Cells were plated to confluency in a fibronectin-coated ECIS 8W10E+ gold electrode chamber slide (Biophysics). Resistance across the monolayer was measured using the Electrical Cell-substrate Impedance System (ECIS) from Applied Biophysics. Cells were allowed to rest for 30 minutes prior to any treatment. Values were normalized against control and quantified.

4.6.6 Apoptosis Induction and Drug Inhibitors

To induce apoptosis via UV-C light, cells were placed into a UV Stratalinker 1800 set to the Autocrosslink set at 400. Inhibition of Rho was done using Y27632 dihydrochloride (Tocris 1254) at a 200μM concentration. Inhibition of the S1P pathways was done using either 10μM JTE-013 (Tocris 2392) or 30μM SKI II (EMD 509106) prior to UV exposure.

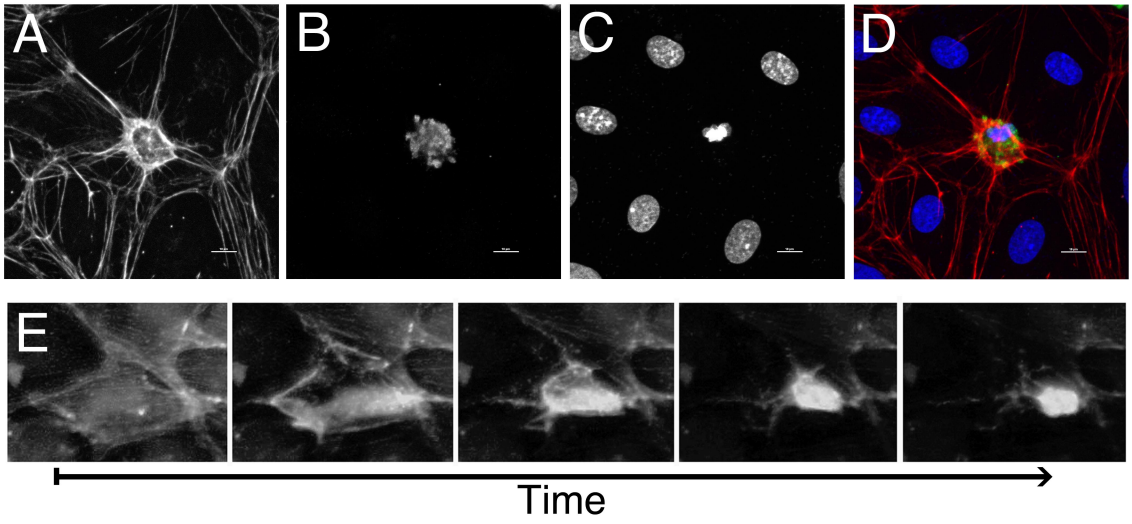

Figure 4.1. Extrusion occurs in the endothelium. A-D. Fluorescent micrographs of an endothelial cell undergoing extrusion. The actin ring can be seen, as labeled with phalloidin (A), closing around a dying cell, as indicated by both active caspase staining (B) and condensed nuclei (C, DAPI). The final panel is a merged image with phalloidin in red, caspase in green, and nuclei in blue. E. Still images taken from a timelapse recording of LifeAct expressing endothelial cell extruding.

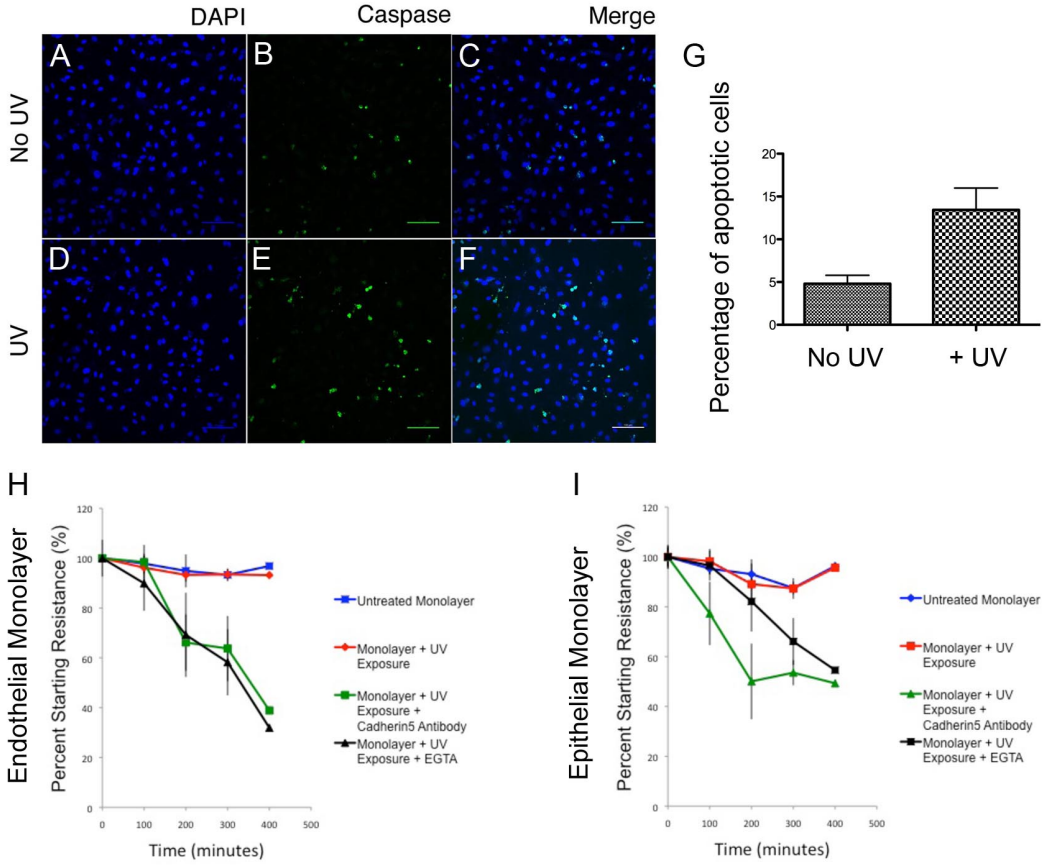

Figure 4.2. Endothelial and epithelial barrier function is maintained during apoptotic stress. A-F. Fluorescent images of apoptosis in an endothelial monolayer. As indicated by nuclear (DAPI, blue; A,D) and caspase (green; B,E) staining. (C,F) are a merged image. G. Quantification of apoptosis as determined by relative fluorescence of caspase staining. H. Transendothelial measurement of resistance, an indicator of barrier function. UV-exposed endothelial cells are able to maintain resistance. Cadherin-5, functional blocking antibody, was used to control for junction disruption. EGTA was used as a positive control. I. The epithelial cell-line, MDCK, displays similar patterns of resistance to that seen in endothelial cells.

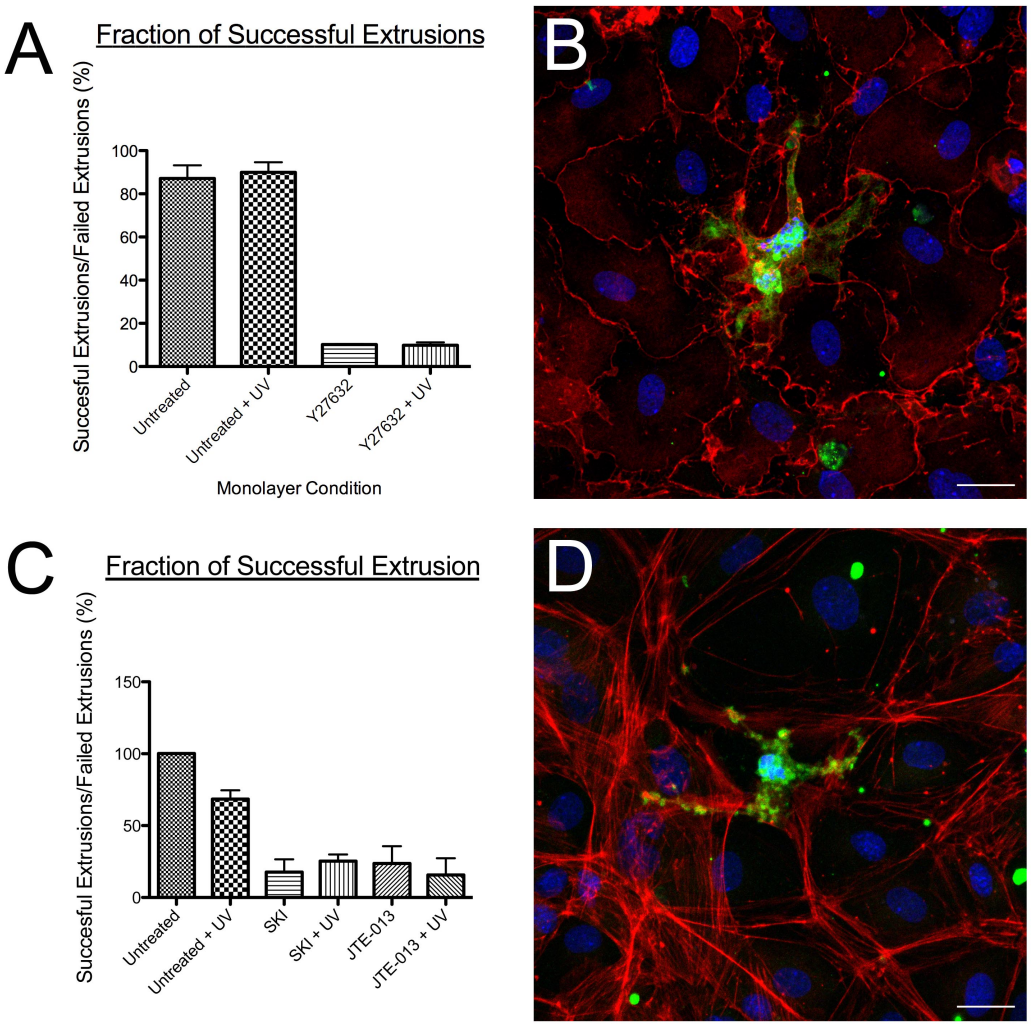

Figure 4.3. Endothelial extrusion uses the S1P-S1P2R-Rho pathway. A,B. Cells treated with Y27632 or sphingosine kinase inhibitor treated remain stuck in the monolayer C,D. Cells were stained for actin (red), caspase (green), and nuclei (DAPI, blue). E. Quantification of Y27632 (50uM) and sphingosine kinase (30uM) inhibitor treated monolayers.

A

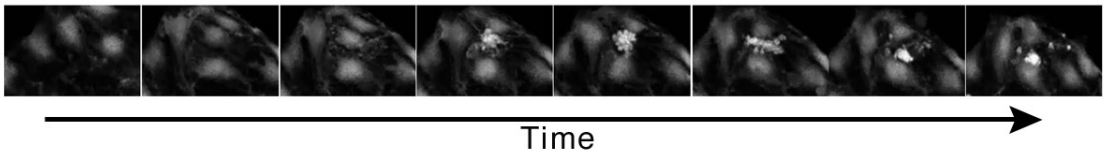

B

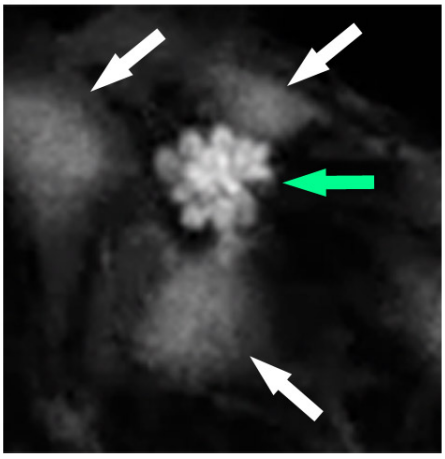

C

# of Fish	# of Extrusions
6	3
4	1
7	3
4	2
9	9
9	14

Figure 4.4. Endothelial extrusion occurs *in vivo.* A. Still images taken from a timelapse recording of a developing CCV in zebrafish with endothelial cells undergoing extrusion. B. Close up of an extrusion still. White arrows indicate neighboring cells while the green arrow indicates cell mid-extrusion. C. Table quantifying the number extrusions per live imaging experiment.

4.7 References

1 Udan, R.S., Culver, J.C. and Dickinson, M.E., J.C.C.a.M.E.D. (2013) Understanding vascular development. *WIREs Dev. Biol.*, **2**, 327-346.

2 Alberts B, Johnson.A., Lewis J, Raff, M., Roberts, K. and Walter, P., (2002). *Molecular Biology of the Cell*. 4th edition. Garland Science, New York, in press.

3 Weis, S.M. and Cheresh, D.A. (2005) Pathophysiological consequences of VEGF-induced vascular permeability. *Nature*, **437**, 497-504.

4 Sprague, A.H. and Khalil, R.A. (2009) Inflammatory cytokines in vascular dysfunction and dascular disease. *Biochem. Pharmacol.*, **78**, 539-552.

5 Rosenblatt J, Raff, M.C. and Cramer, L.P. (2001) An epithelial cell destined for apoptosis signals its neighbors to extrude it by an actin- and myosin-dependent mechanism. *Curr. Biol.*, **11**, 1847-1857.

6 Eisenhoffer, G.T., Loftus, P.D., Yoshigi, M., Otsuna, H., Chien, C.B., Morcos, P.A. and Rosenblatt, J. (2012) Crowding induces live cell extrusion to maintain homeostatic cell numbers in epithelia. *Nature*, **484**, 546-549.

7 Andrade, D. and Rosenblatt, J. (2011) Apoptotic regulation of epithelial cellular extrusion. *Apoptosis*, **16**, 491-501.

8 Slattum, G., McGee, K.M. and Rosenblatt, J. (2009) P115 RhoGEF and microtubules decide the direction apoptotic cells extrude from an epithelium. *J. Cell Biol.*, **186**, 693-702.

9 Gu, Y., Forostyan, T., Sabbadini, R. and Rosenblatt, J. (2011) Epithelial cell extrusion requires the sphingosine-1-phosphate receptor 2 pathway. *J. Cell Biol.*, **4**, 667-676.

10 Lorenz, J.N., Arend, L.J., Robitz, R., Paul, R.J. and MacLennan, A.J. (2007) Vascular dysfunction in S1P2 sphingosine 1-phosphate receptor knockout mice. *Am. J. Phys.*, **292**, 440-446.

11 Skoura, A. and Hla, T. (2009) Regulation of vascular physiology and pathology by the S1P2 receptor subtype. *Cardiovasc. Res.*, **82**, 221-228.

12 Karmina, K. and Herbomel, P. (2010) Blood stem cells emerge from aortic endothelium by a novel type of cell transition. *Nature*, **464**, 112-115.

CHAPTER 5

CONCLUSION

Taken together, the work presented in this dissertation provides advancements in the fields of Cerebral Cavernous Malformation and endothelial cell biology. First, using a novel mouse model of CCM, we describe the early morphological onset of CCM lesions within the retina and present two novel defects, the first being endothelial hypersprouting in the retina, which precedes lesion formation, and the second being an impaired endothelial response to flow. Both inform us about the initial defects that contribute to lesion formation and focus on primary disease cause rather than on later effects. Second, we go on to demonstrate that a second genetic hit is not adequate for adult lesion onset and that an additional environmental hit is needed. In conjunction with our finding that lesions develop in a stereotypical pattern, this calls into question the two-hit hypothesis in CCM. Finally, we go on to examine barrier function and define the existence of endothelial cellular extrusion, which could potentially be a contributing factor to the leak observed in CCM.

Several questions remain to be addressed as each chapter has opened up new directions to be investigated. Questions remain as to the exact mechanism responsible for the impaired flow response and the signaling cascades disrupted during angiomorphogenesis. Determining if there is a minimum or maximum flow rate

threshold that cells respond to would provide insight into arteriovenous differentiation. In addition, changes in the downstream signaling upon flow stimulation needs to be studied, for example, changes in proliferation or apoptosis. Furthermore, work needs to be done to determine if response to flow can be influenced by environmental factors, or vice versa. Determining which environmental factors can lead to adult CCM onset is also a question open for investigation as several pathways have been implicated in CCM pathogenesis. How these pathways interconnect and whether the resulting defects, such as vascular leak, could contribute to the environmental hits associated with late onset disease remains to be seen. Lastly, could defective endothelial extrusion contribute to the formation of CCM? Rho signaling is critical for extrusion, considering that Rho is dysregulated when CCM2 is lost, which suggests that the barrier function provided by extrusion could be disrupted in the disease. More work is needed to determine if loss of the CCM genes disrupts the process of extrusion and if that contributes to vascular leak. In the end, each of these studies is a reminder that rarely is a disease ever a symptom of a singular, concrete defect. Rather, diseases arise from a defect that cascades into other defects until a single stream has flooded into an ocean.